



Measurement of the nuclear modification factor for muons from charm and bottom hadrons in Pb+Pb collisions at 5.02 TeV with the ATLAS detector



The ATLAS Collaboration*

ARTICLE INFO

Article history:

Received 2 September 2021

Received in revised form 16 February 2022

Accepted 2 April 2022

Available online 6 April 2022

Editor: M. Doser

ABSTRACT

Heavy-flavour hadron production provides information about the transport properties and microscopic structure of the quark–gluon plasma created in ultra-relativistic heavy-ion collisions. A measurement of the muons from semileptonic decays of charm and bottom hadrons produced in Pb+Pb and pp collisions at a nucleon–nucleon centre-of-mass energy of 5.02 TeV with the ATLAS detector at the Large Hadron Collider is presented. The Pb+Pb data were collected in 2015 and 2018 with sampled integrated luminosities of $208 \mu\text{b}^{-1}$ and $38 \mu\text{b}^{-1}$, respectively, and pp data with a sampled integrated luminosity of 1.17pb^{-1} were collected in 2017. Muons from heavy-flavour semileptonic decays are separated from the light-flavour hadronic background using the momentum imbalance between the inner detector and muon spectrometer measurements, and muons originating from charm and bottom decays are further separated via the muon track's transverse impact parameter. Differential yields in Pb+Pb collisions and differential cross sections in pp collisions for such muons are measured as a function of muon transverse momentum from 4 GeV to 30 GeV in the absolute pseudorapidity interval $|\eta| < 2$. Nuclear modification factors for charm and bottom muons are presented as a function of muon transverse momentum in intervals of Pb+Pb collision centrality. The bottom muon results are the most precise measurement of b quark nuclear modification at low transverse momentum where reconstruction of B hadrons is challenging. The measured nuclear modification factors quantify a significant suppression of the yields of muons from decays of charm and bottom hadrons, with stronger effects for muons from charm hadron decays.

© 2022 The Author(s). Published by Elsevier B.V. This is an open access article under the CC BY license (<http://creativecommons.org/licenses/by/4.0/>). Funded by SCOAP³.

1. Introduction

Quark–gluon plasma (QGP) is a state of matter in which the quarks and gluons are deconfined from colour-neutral hadronic states. Ultra-relativistic collisions of large nuclei create nuclei-sized droplets of QGP at temperatures in excess of 300–500 MeV [1,2]. These droplets exist for a mere 10^{-23} seconds and hence there is no way to fire an external probe at the droplet to investigate its properties. Instead, the probes must be generated in the collision itself and then interact with the droplet. Interactions with the QGP, both radiative and collisional, may provide key information regarding the properties and constituents of the QGP [3]. Specifically, the balance of radiative and collisional energy transfer depends on the mass of the constituents [4,5]. Heavy quarks, charm and bottom, have masses much larger than the droplet temperature. Thus, they are produced in the initial collision via high-momentum-transfer interactions between incident quarks and gluons. The strong-force interactions conserve the quantum numbers associated with the

charm and bottom quarks. Thus, once created, these quarks can have substantial modifications to their momentum distributions when traversing the QGP, but they cannot be destroyed. In addition, radiative energy loss is suppressed for heavy quarks by the so-called ‘dead-cone effect’ [6], i.e. gluon radiation is suppressed at angles smaller than the quark's mass to energy ratio. A key to constraining the relative contribution of radiative energy loss is to measure the modification of the momentum distributions for charm and bottom quarks separately, since the dead-cone effect will be more pronounced for bottom quarks than for charm quarks at the same momentum.

There are numerous publications detailing the modifications of momentum distributions of heavy-flavour hadrons measured in heavy-ion collisions via direct reconstruction and via decay leptons in heavy-ion collisions at the Relativistic Heavy Ion Collider (RHIC) [7] and the Large Hadron Collider (LHC) [8] – current measurements and theory calculations are reviewed in Refs. [9,10]. In nucleus–nucleus (A+A) collisions, each event is described by its centrality, which reflects the overlap of the colliding nuclei. The geometry of each event is calculated using a Monte Carlo (MC) Glauber model – for details see Ref. [11]. The modification to par-

* E-mail address: atlas.publications@cern.ch.

particle yields in A+A collisions relative to pp collisions is quantified by a nuclear modification factor R_{AA} defined as:

$$R_{AA} = \frac{N_{AA}/N_{\text{evt}}}{\langle T_{AA} \rangle \times \sigma_{pp}}, \quad (1)$$

where N_{AA} is the number of observed particles of interest in Pb+Pb collisions, N_{evt} is the number of minimum-bias Pb+Pb events, $\langle T_{AA} \rangle$ is the average value of the nuclear thickness function, and σ_{pp} is the particle production cross section in pp collisions at the same collision energy. If R_{AA} equals unity, the production in A+A collisions is the same as in pp collisions but scaled up by the larger parton-parton luminosity, while $R_{AA} < 1$ indicates a suppression.

The nuclear modification factors for inclusive ‘heavy-flavour muons’ (mostly muons from D and B meson semileptonic decays) have been measured in Pb+Pb collisions at $\sqrt{s_{NN}} = 2.76$ TeV by the ATLAS experiment [12] and the ALICE experiment [13]. The ALICE experiment measured the nuclear modification factor for inclusive heavy-flavour electrons at the same energy [14,15] and also at $\sqrt{s_{NN}} = 5.02$ TeV [16]. Nuclear modification factors for charm hadrons D^0 , D_s , D_s^* , and Λ_c have been measured by the CMS [17] and ALICE [18,19] experiments in Pb+Pb collisions at $\sqrt{s_{NN}} = 5.02$ TeV, and by the STAR [20–23] experiment in Au+Au collisions at a lower energy of $\sqrt{s_{NN}} = 200$ GeV. These measurements indicate significant suppression for heavy-flavour hadrons in Pb+Pb collisions. At transverse momentum (p_T) greater than 4 GeV, the prompt- D^0 R_{AA} is found to be consistent within the uncertainties with the R_{AA} of inclusive charged particles (dominated by π), while at lower p_T values D^0 mesons have a smaller suppression (larger R_{AA}) compared to charged particles, as expected theoretically from the dead-cone effect.

The measurement presented here follows the previous ATLAS measurement of muons originating from heavy-flavour hadron decays in Pb+Pb collisions at $\sqrt{s_{NN}} = 2.76$ TeV [12]. This Letter, based on the higher number of events in the combined 2015 and 2018 Pb+Pb datasets and the 2017 pp dataset at 5.02 TeV, extends results to the transverse momentum range $4 < p_T < 30$ GeV, and more importantly, further separates inclusive heavy-flavour muons into contributions from charm hadron decays (charm muons) and bottom hadron decays (bottom muons). The charm and bottom contribution separation is based on the muon track’s transverse impact parameter, similar to the method used in previous ATLAS measurements [24,25]. Results for charm and bottom muon cross sections in pp collisions are shown as a function of muon p_T and compared with perturbative QCD calculations. The nuclear modification factor is presented as a function of muon p_T in various Pb+Pb centrality intervals. Finally, the R_{AA} measurements, along with a previous measurement of the heavy-flavour muon momentum anisotropies [25], are compared with the expectations from theoretical calculations. The R_{AA} value quantifies the average energy loss, and the azimuthal anisotropy, v_2 [25], at high p_T , quantifies the azimuthal angle dependence of energy loss. Simultaneous constraints on R_{AA} and v_2 for the same final state are important in distinguishing the relative impacts of different heavy-quark energy loss mechanisms and in understanding the influence of the initial QGP droplet geometry on the resulting evolution of kinematics of heavy-flavour quarks in the medium.

2. ATLAS detector

The ATLAS detector [26–28] at the LHC covers nearly the entire solid angle around the collision point.¹ It consists of an inner

tracking detector surrounded by a thin superconducting solenoid, electromagnetic and hadronic calorimeters, and a muon spectrometer incorporating three large superconducting toroidal magnets with eight coils each. The inner-detector system (ID) is immersed in a 2 T axial magnetic field and provides charged-particle tracking in the range $|\eta| < 2.5$.

The high-granularity silicon pixel detector covers the vertex region and typically provides four measurements per track, with the first hit typically in the insertable B-layer installed before Run 2 [27,28]. It is followed by the silicon microstrip tracker which usually provides eight measurements per track. These silicon detectors are complemented by the transition radiation tracker (TRT), which enables radially extended track reconstruction up to $|\eta| = 2.0$.

The calorimeter system covers the pseudorapidity range $|\eta| < 4.9$. Within the region $|\eta| < 3.2$, electromagnetic calorimetry is provided by barrel and endcap high-granularity lead/liquid-argon (LAr) calorimeters, with an additional thin LAr presampler covering $|\eta| < 1.8$ to correct for energy loss in material upstream of the calorimeters. Hadronic calorimetry is provided by the steel/scintillator-tile calorimeter, segmented into three barrel structures within $|\eta| < 1.7$, and two copper/LAr hadronic endcap calorimeters. The solid angle coverage is completed with forward copper/LAr and tungsten/LAr calorimeter modules (FCal), covering the forward regions of $3.1 < |\eta| < 4.9$, optimized for electromagnetic and hadronic measurements respectively. The minimum-bias trigger scintillators detect charged particles over $2.07 < |\eta| < 3.86$ using two hodoscopes of 12 counters positioned at $z = \pm 3.6$ m. The zero-degree calorimeters (ZDC) measure neutral particles at pseudorapidities $|\eta| \geq 8.3$ and consist of layers of alternating quartz rods and tungsten plates.

The muon spectrometer (MS) comprises separate trigger and high-precision tracking chambers measuring the deflection of muons in a magnetic field generated by superconducting air-core toroids. The field integral of the toroids ranges between 2.0 and 6.0 Tm across most of the detector. A set of precision chambers covers the region $|\eta| < 2.7$ with three layers of monitored drift tubes, complemented by cathode-strip chambers in the forward region, where the background is highest. The muon trigger system covers the range $|\eta| < 2.4$ with resistive-plate chambers in the barrel, and thin-gap chambers in the endcap regions. Events of interest are selected to be recorded by the first-level trigger (L1) system implemented in custom hardware, followed by selections made by algorithms implemented in software in the high-level trigger (HLT) [29]. The first-level trigger selects events from the 40 MHz bunch crossings at a rate below 100 kHz (75 kHz) for pp (Pb+Pb) collisions, and the high-level trigger reduces the average event output rate to about 1.2 kHz for recording. An extensive software suite [30] is used for real and simulated data reconstruction and analysis, for operation and in the trigger and data acquisition systems of the experiment.

3. Event selection

The pp data used in this analysis were recorded with the ATLAS detector in 2017, while the Pb+Pb data were recorded in 2015 and 2018. Both the pp and Pb+Pb events were selected online using a trigger that requires a muon at the L1 and HLT with a p_T larger than 4 GeV [29,31]. After selecting run periods when the detector subsystems were operational and taking into account the fraction of the total luminosity sampled by the triggers, the datasets used

¹ ATLAS uses a right-handed coordinate system with its origin at the nominal interaction point (IP) in the centre of the detector and the z -axis along the beam pipe. The x -axis points from the IP to the centre of the LHC ring, and the y -axis

points upwards. Cylindrical coordinates (r, ϕ) are used in the transverse plane, ϕ being the azimuthal angle around the z -axis. The pseudorapidity is defined in terms of the polar angle θ as $\eta = -\ln \tan(\theta/2)$. Angular distance is measured in units of $\Delta R \equiv \sqrt{(\Delta\eta)^2 + (\Delta\phi)^2}$.

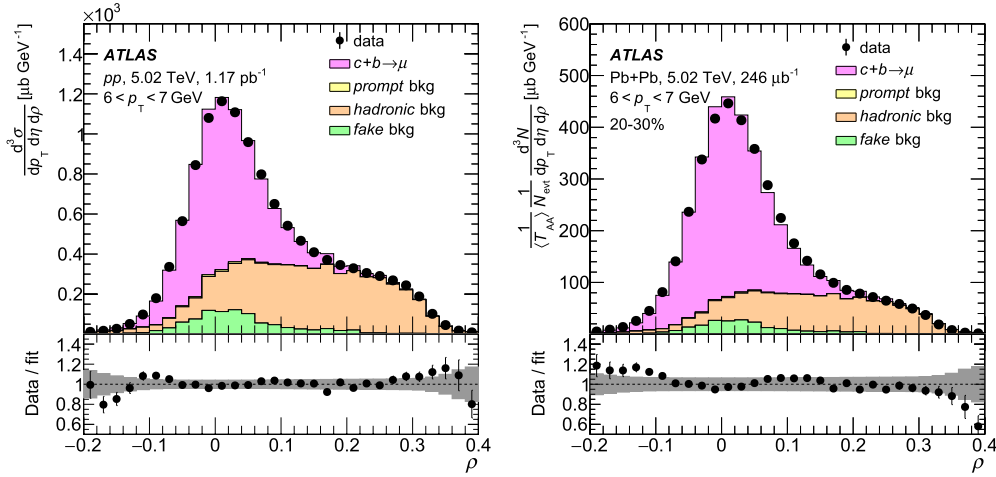


Fig. 1. Fit results of the ρ distribution for muons with $6 < p_T < 7$ GeV in pp collisions (left) and in Pb+Pb collisions with 20–30% centrality (right). The ratios of the data to fit results are shown in the lower panels. The prompt-muon background contributions are very small in the fitted muon kinematic region. The grey bands in the lower panels indicate the statistical and systematic uncertainties combined in quadrature.

in the analysis correspond to integrated luminosities of 1.17 pb^{-1} for pp data, $208 \text{ } \mu\text{b}^{-1}$ for 2015 Pb+Pb data, and $38 \text{ } \mu\text{b}^{-1}$ for 2018 Pb+Pb data. The 2017 pp data, with a small average number of interactions per bunch crossing in the range from 0.4 to 4, were collected to serve as the baseline for Pb+Pb collision measurements at the same centre-of-mass energy per nucleon pair. Only a small fraction of events from the 2018 Pb+Pb data was recorded by the low p_T muon trigger used in this analysis. Other muon triggers in the 2018 Pb+Pb data were studied and improved statistical uncertainties while increasing systematic uncertainties, and are thus not incorporated. The 2015 and 2018 results are consistent and thus combined in these results. The selected Pb+Pb events are further required to satisfy offline minimum-bias Pb+Pb collision criteria, identical to those used in Ref. [25]. This additional requirement identifies and rejects 0.2% of the selected events as pile-up events, based on a combination of the total transverse energy measured in the FCal, denoted by ΣE_T^{FCal} , and the ZDC energy.

The centrality of each Pb+Pb event is characterized by its ΣE_T^{FCal} value. For the results shown here, the minimum-bias ΣE_T^{FCal} distribution is divided into percentiles ordered from the most central (large ΣE_T^{FCal} , small impact parameter) to the most peripheral (small ΣE_T^{FCal} , large impact parameter): 0–10%, 10–20%, 20–30%, 30–40%, and 40–60%. The interval 0–100% corresponds to the total Pb+Pb inelastic cross section [32]. An MC Glauber [11] model is used to calculate $\langle T_{AA} \rangle$ for each centrality interval [33].

Muons with $4 < p_T < 30$ GeV and $|\eta| < 2$ reconstructed in both the ID and the MS are selected and required to pass ‘medium’ selection requirements, detailed in Ref. [34]. Selected muons are required to be matched with an online muon candidate that fires the event trigger. Each muon is assigned a weight which is the inverse of the product of the reconstruction and trigger efficiencies, evaluated for muons as a function of their kinematic variables, and in the case of Pb+Pb data as a function of centrality as well.

The muon reconstruction and identification efficiency is factorized as the product of the individual reconstruction efficiencies in the ID and MS, where the ID and MS matching efficiency is included in the MS efficiency. The ID and MS efficiencies in pp collisions are determined in the large pp dataset collected in 2017 at $\sqrt{s} = 13$ TeV, using the tag-and-probe method on $J/\psi \rightarrow \mu^+ \mu^-$ events as detailed in Ref. [34]. They are applied to the pp data at $\sqrt{s} = 5.02$ TeV used in this analysis, in fine intervals of muon p_T and η . The difference between the muon reconstruction efficiencies at $\sqrt{s} = 5.02$ TeV and $\sqrt{s} = 13$ TeV due to different pile-up contributions and multiplicities is found to be negligible [34]. The

MS efficiencies obtained from pp and Pb+Pb data collected in the same year show no significant difference. Thus, the MS efficiencies for 2015 and 2018 Pb+Pb data are obtained from the large pp datasets at $\sqrt{s} = 13$ TeV in the corresponding years in fine intervals of muon p_T and η . The resulting MS efficiency plateaus at 97% at $p_T > 7$ GeV. The ID efficiency in Pb+Pb events is obtained from Pb+Pb data using the same $J/\psi \rightarrow \mu^+ \mu^-$ tag-and-probe method in intervals of muon p_T and η . The measured Pb+Pb ID efficiency is about 98% with the efficiency in 2018 being 3% lower than that in 2015 at $1 < |\eta| < 2$ independent of p_T , while no difference between 2015 and 2018 is observed at $|\eta| < 1$. No centrality dependence is observed for MS and ID efficiencies for muons in Pb+Pb collisions.

The initial estimations of the muon trigger efficiency are obtained from $J/\psi \rightarrow \mu^+ \mu^-$ PYTHIA8 [35] simulations in fine intervals of muon p_T and η using the tag-and-probe method [31]. All generated events were passed through a GEANT4 simulation [36,37] of the ATLAS detector under the same conditions as present during data-taking and were digitized and reconstructed in the same way as the data. The same simulated trigger efficiency is used in pp and Pb+Pb data. Relative efficiency differences between simulations and data and between pp and Pb+Pb collisions are covered by additional corrections described as follows. Mis-modelling of the trigger performance in simulation, quantified by the ratio of measured efficiencies in data and the simulations, is accounted for by applying a multiplicative correction not exceeding 10%. To account for the different online muon momentum scale in pp and Pb+Pb data, as well as the slightly different trigger performance in 2015 and 2018, an additional correction factor, determined by the Pb+Pb to pp data-driven efficiency ratio, is applied to Pb+Pb data as a function of muon p_T and η , the centrality, and the year of Pb+Pb data-taking.

4. Signal extraction

As detailed in previous ATLAS publications [12,24,25,38], the background contributions in the selected muon samples (labelled ‘bkg’ in Figs. 1 and 2) have three components. The first one is called the ‘prompt-muon background’ and includes contributions from decays of non-open-heavy-flavour particles such as direct quarkonia, low-mass resonances, τ -leptons, and massive electroweak W/Z bosons. The second component is the ‘hadronic background’ resulting from π and K decaying into muons in the volume of the ID or punching through the calorimeter. The last

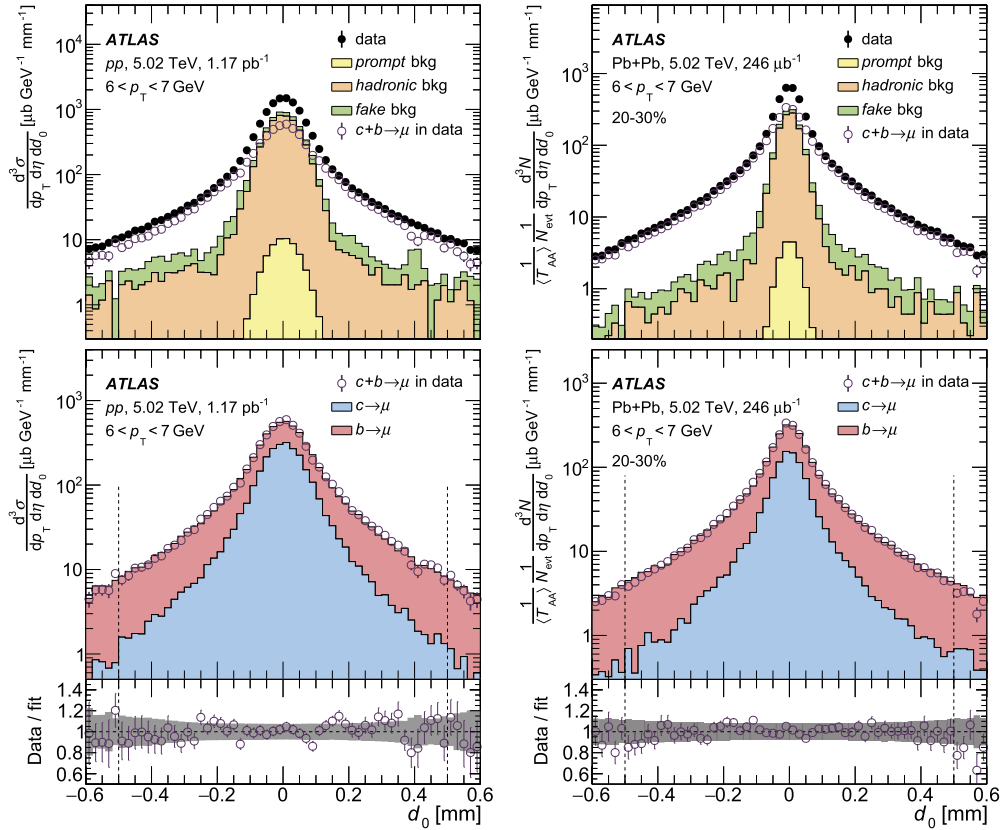


Fig. 2. (Top) d_0 templates for different background contributions, and data d_0 distributions before (solid points) and after (open points) background subtraction for muons with $6 < p_T < 7$ GeV in pp collisions (left) and in Pb+Pb collisions with 20–30% centrality (right). (Bottom) Fit results of the background-subtracted d_0 distribution for muons with $6 < p_T < 7$ GeV in pp collisions (left) and in Pb+Pb collisions with 20–30% centrality (right). The vertical dashed lines indicate the d_0 range, $|d_0| < 0.5$ mm, used in the fit procedure. Data to fitted result ratios are shown in the bottom panels. The grey bands indicate the statistical and systematic uncertainties combined in quadrature.

component is from random combinations of uncorrelated track segments from the ID and MS, called the ‘fake-muon background’. The prompt-muon background, expected to be small compared to signal muons, is estimated in simulations. These simulations are scaled to match existing measurements of different background sources under consistent fiducial selections. The main prompt-muon background for muons with $20 < p_T < 30$ GeV is from W decays, and is approximately 3% in pp collisions at 10% (5%) in 0–10% (40–60%) Pb+Pb collisions based on previous ATLAS measurements [39,40]. Hadronic and fake-muon backgrounds are subtracted from the signal muons by fitting the muon momentum imbalance, $\rho = (p^{\text{ID}} - p^{\text{MS}})/p^{\text{ID}}$, where p^{ID} is the muon momentum measured in the ID, and p^{MS} is that measured in the MS corrected for the energy loss inside the calorimeter. The ρ distribution shapes of hadronic and fake-muon backgrounds are extracted from simulations while their yields are determined from the fit procedure.

The prompt-muon background contribution in pp events is estimated from PYTHIA8 simulations of prompt J/ψ , $\psi(2S)$, and $\Upsilon(nS)$ production based on a non-relativistic QCD colour-octet model [41], and from W and Z production simulated with the POWHEG Box v2 generator [42] interfaced to the PYTHIA8 parton shower model. The CT10 PDF set [43] was used in the matrix element, while the CTEQ6L1 PDF set [44] was used for the modelling of non-perturbative effects in the initial-state parton shower. The simulated prompt-muon background processes are all scaled by process-dependent single scaling factors to match previous ATLAS measurements in pp collisions at $\sqrt{s} = 5.02$ TeV [39,45]. Other contributions from low-mass resonances and τ -leptons in the measured muon p_T range are found to be less than 1% [24,38] and are neglected in this analysis. In Pb+Pb collisions, the esti-

mated prompt-muon background rates take into account nuclear modifications measured in Refs. [40,46–48].

Muons from hard scattering have a symmetric ρ distribution peaked at zero, while the hadronic background has a broader ρ distribution and the peak shifted toward higher values. This change in shape is due to differences between the actual energy loss of this background and the estimated energy loss based on muon simulations. Only energy loss of muons is properly corrected for and added to the MS momentum measurement. The different shapes of the ρ distributions for the hadronic background and the other muons allow the hadronic background to be isolated using a template-fitting procedure [24,25]. The yields of inclusive heavy-flavour muons and hadronic background muons are extracted from the ρ template fit. The templates for the charm and bottom muon ρ distributions are determined from multijet hard-scattering PYTHIA8 pp collision events at $\sqrt{s} = 5.02$ TeV filtered for the presence of a generator-level muon produced with parameter values as in the A14 tune [49] and using the NNPDF23LO parton distribution functions [50]. The templates for the charm and bottom muon ρ distributions (and track transverse impact parameter, d_0 , distributions, described below) in multijet hard-scattering QCD PYTHIA8 samples are found to be identical to those from non-diffractive QCD PYTHIA8 samples, while hard-scattering QCD PYTHIA8 samples have much higher muon filter efficiency. The ρ templates for the prompt-muon background are obtained from the simulation procedure described in the previous paragraph. The hadronic background and fake-muon ρ templates are obtained from non-diffractive QCD simulations of pp collisions at $\sqrt{s} = 5.02$ TeV in PYTHIA8, with the A14 tune and NNPDF23LO parton distribution functions. The fake-muon contribution is fixed relative to the hadronic background, with the ratio obtained from

simulations. The momenta of the reconstructed muons selected in PYTHIA8 simulations are calibrated to match the muon momentum response in pp and Pb+Pb data. The calibration is performed via shift and smearing parameters [25] determined from the invariant mass response in $J/\psi \rightarrow \mu^+\mu^-$ events. The same calibration is applied to all muon candidates including those from background contributions. Alternative calibrations for background contributions are used for the systematic uncertainty evaluation.

Examples of the ρ template fit are shown in Fig. 1 for muons with $6 < p_T < 7$ GeV in pp collisions and 20–30% centrality Pb+Pb collisions. The signal muon ρ distribution shape shows no obvious dependence on muon p_T , but is found to be broader in the more forward pseudorapidity region and more central Pb+Pb collisions, both due to poorer muon momentum resolution in the ID. The hadronic background ρ distribution becomes broader at higher p_T and in more central collisions.

Charm and bottom muons are further separated using the muon track's transverse impact parameter, d_0 , which is calculated relative to the beam spot [51]. Due to the different lifetimes of charm and bottom hadrons (approximately 1.5×10^{-12} s for B mesons, 1.0×10^{-12} s for D^+ and 0.4×10^{-12} s for D^0 mesons), the corresponding muons have different d_0 distributions, and their fractional contributions can be extracted using a template-fitting procedure. Background contributions are subtracted from data distributions of d_0 as shown in the upper panels in Fig. 2. For each of the three background sources, the d_0 shape is determined in simulations. In pp data analysis, the d_0 shape templates of various background sources are obtained from the PYTHIA8 simulations used to build the ρ templates. In Pb+Pb data analysis, the same PYTHIA8 events overlaid with minimum-bias Pb+Pb events collected in 2015 are used to build the background d_0 templates to approximate background distributions in Pb+Pb collisions. The d_0 distributions from high-quality prompt tracks in simulations and 2018 Pb+Pb data are smeared to match those in 2015 Pb+Pb data. The prompt-muon background d_0 distribution normalization is constrained by the yield estimates from MC simulations. The hadronic and fake-muon background d_0 distribution normalization factors are extracted from the ρ template fit. The signal muon d_0 distribution in Pb+Pb data is narrower than in pp data because of a smaller transverse beam size. The background d_0 distribution becomes moderately narrower with increasing p_T and shows no evident centrality dependence. After subtraction, the remaining d_0 distribution in data contains only contributions from heavy-flavour muons.

The d_0 fit is performed in the range of $|d_0| < 0.5$ mm as events with $|d_0| > 0.5$ mm are statistically limited in both data and simulations and have little sensitivity to the charm muon contribution. For pp data, the charm and bottom muon d_0 templates are obtained from the muon-filtered multijet PYTHIA8 simulations at $\sqrt{s} = 5.02$ TeV, as done for ρ templates. Bottom muons contain the $b \rightarrow c \rightarrow \mu$ cascade contribution. The d_0 distributions of signal muons show no obvious dependence on the muon p_T , but they become broader with increasing parent B and D meson p_T . The simulated samples from PYTHIA8 are reweighted to match the inclusive B and D meson p_T spectra from fixed-order next-to-leading-log (FONLL) resummation calculations [52,53]. The charm and bottom baryon-to-meson ratios in the simulations are corrected to match the measured values in Refs. [54,55]. The baryon-to-meson ratio is treated the same in pp and Pb+Pb, and allowed to vary independently for each system by a factor of two, based on values reported in Ref. [56], in determining systematic uncertainties. The yield of D^+ relative to D^0 is corrected to match the measured value in Refs. [57,58]. In the Pb+Pb analysis, the charm and bottom muon d_0 templates are obtained from the pp PYTHIA8 simulations overlaid with minimum-bias Pb+Pb events from 2015, similar to what is done for the background d_0 templates. Besides

the FONLL resummation and baryon-to-meson corrections as applied in pp collisions, an additional correction is applied to match the modified charm and bottom hadron p_T spectra measured in Pb+Pb collisions by ALICE [18] and CMS [17]. Examples of d_0 template fits for muons with $6 < p_T < 7$ GeV are shown in Fig. 2 for pp collisions and 20–30% centrality Pb+Pb collisions. The relative fractions of charm and bottom muons are extracted from the d_0 template fit.

5. Systematic uncertainties

Systematic uncertainties associated with the various steps of the analysis are assessed. The measured cross section in pp collisions, per-event yields in Pb+Pb collisions and R_{AA} are recalculated by systematically varying the effect of each source of uncertainty and then compared with the nominal results. The resulting difference is assigned as a systematic uncertainty. Each group of systematic uncertainties described in the following subsections are considered as uncorrelated, and are therefore summed in quadrature. Some sources of systematic uncertainties that are correlated between pp and Pb+Pb collisions partially cancel out in R_{AA} .

5.1. Muon correction uncertainties

The systematic uncertainties from the muon reconstruction efficiency and muon trigger efficiency corrections for pp collisions are dominated by the uncertainty in determining these efficiencies in data with the tag-and-probe method. These are evaluated following the procedures in previous ATLAS measurements [31, 34], including variations in the tag-and-probe efficiency extraction method, online-offline matching requirement, and muon purity in the selected sample. The Pb+Pb efficiency is affected by the systematic uncertainty sources mentioned above, due to the use of the pp efficiency in the factorized treatment. An additional uncertainty in Pb+Pb is associated with the determination of the ID reconstruction efficiency in data using the tag-and-probe method. Uncertainties in the trigger efficiency correction are determined from the Pb+Pb to pp efficiency ratio and residual discrepancies between fully corrected Pb+Pb muon spectra measured in the 2015 and 2018 data-taking periods. Apart from specific Pb+Pb uncertainties, other uncertainties are correlated between collision systems and thus cancel out in R_{AA} .

5.2. Background removal uncertainties

The systematic uncertainty in the momentum imbalance templates includes the effect of the uncertainty in the muon momentum calibration parameters, the uncertainty due to the dedicated hadronic-background calibration, and the uncertainty due to ρ - d_0 correlation in the hadronic background. Charm muon yields are more sensitive to the background removal procedure as charm muons have narrower d_0 distributions around 0 where the background contamination is large. The systematic uncertainties in the calibration parameters, which originate from the uncertainty in the determination of $J/\psi \rightarrow \mu^+\mu^-$ invariant mass [59], contribute 3% relative uncertainty to the final charm muon yields and 1% to the bottom muon yields. Since the hadronic background could have a different momentum scale than that for real muons, the results are also examined using a data-driven hadronic-background momentum calibration in the background-dominated region $\rho > 0.2$. The difference is included as a systematic uncertainty which is about 10% (4%) for charm (bottom) muon yields at low p_T and decreases with increasing p_T . To account for the small ρ - d_0 correlation in hadronic background, the corresponding ρ templates in different d_0 selections are used and the resulting difference is assigned as an additional systematic uncertainty. The relative uncertainty due

Table 1

Contributions to systematic uncertainties given in percent for the cross section in pp , yields in Pb+Pb, and nuclear modification factor of charm and bottom muons. Ranges indicate the minimum and maximum systematic uncertainties found in all muon p_T bins and centralities for a given source.

Source	σ_{pp} [%]		N_{AA} [%]		R_{AA} [%]	
	$c \rightarrow \mu$	$b \rightarrow \mu$	$c \rightarrow \mu$	$b \rightarrow \mu$	$c \rightarrow \mu$	$b \rightarrow \mu$
Muon efficiency	0.5–1.0	0.4–0.6	0.6–16	0.3–16	0.3–16	0.2–16
Background removal	4.3–12	0.8–3.8	2.5–30	1.0–5.1	1.9–27	0.5–4.7
Charm–bottom separation	4.5–9.8	3.2–8.0	9.2–37	6.2–16	5.1–23	4.1–13
Global normalization	1.6	1.6	0.9–4.6	0.9–4.6	1.8–4.9	1.8–4.9
Total systematic uncertainty	5.8–13	3.1–7.4	10–47	6.9–19	6.5–35	5.4–18

to the background ρ - d_0 correlation is about 3% for charm muon yields and less than 1% for bottom muon yields. The ρ -template-related systematic uncertainties are treated as correlated between pp and Pb+Pb data, and partially cancel out in R_{AA} .

In the analysis, the size of each prompt-muon background contribution is held at a fixed value obtained from PYTHIA8 simulations scaled to match existing measurements. To assess the associated uncertainty, the pp and Pb+Pb analyses are repeated while varying the estimated sizes of the different prompt-muon contributions by the corresponding experimental uncertainties in their production rates [39,45] and R_{AA} values [40,46–48]. The sensitivity to the fake-muon rate estimation is evaluated by varying the fake-muon candidate definition in simulations with different truth-level and reconstruction-level objects matching criteria. The resulting variation of the fake-muon rate is about 20–40%, and produces 5% variations, on average, in the measured charm and bottom yields. The fake-muon systematic uncertainty is assumed to be uncorrelated between the pp and Pb+Pb results.

5.3. Charm–bottom separation uncertainties

The systematic uncertainties in the impact parameter template, that are common for pp and Pb+Pb results, include several components. Uncertainties in the FONLL calculations are evaluated based on Ref. [52,53]. Uncertainties coming from baryon-to-meson ratio mis-modelling correction measurements published in Ref. [54,55]. Uncertainties in D^+/D^0 mis-modelling correction are based on reported uncertainties in Ref. [60,61]. They are propagated to the pp and Pb+Pb results, and are treated as correlated between the pp and Pb+Pb results. The muon p_T spectra predicted by FONLL calculations are weighted to match the measured charm and bottom muon spectra reported in this Letter. The resulting weighting factors are used to adjust signal d_0 templates to quantify the bias due to observed mis-modelling in the FONLL calculations. The resulting difference of 1–5% in the muon yields is assigned as an additional uncertainty and is treated as correlated between the pp and Pb+Pb results. Uncertainties in the nuclear modification factor for parent hadrons in Pb+Pb are propagated using the experimental uncertainties in D and B meson R_{AA} values from Refs. [17,18]. Minimum-bias Pb+Pb events collected in 2018, instead of 2015 events, are used to overlay with PYTHIA8 simulations to test the sensitivity to slightly different overlay conditions. Resulting changes in the muon yields due to different overlay conditions are assigned as a systematic uncertainty in the Pb+Pb results. Uncertainties in the determination of d_0 shift and smearing parameters are found to have a negligible impact, less than 0.5%, on the extracted charm and bottom yields.

5.4. Global normalization uncertainties

In the 2017 pp data, the LUCID-2 detector [62] is used for the primary luminosity measurement. The uncertainty in the integrated luminosity is derived using the methods described in

Ref. [63], and is 1.6%. For Pb+Pb collisions, the systematic uncertainty in $\langle T_{AA} \rangle$ is estimated by varying the MC Glauber model parameters as detailed in Ref. [33].

5.5. Uncertainty summary

Table 1 summarizes relative uncertainties in the measurement of charm and bottom muon production in pp and Pb+Pb collisions, and in the nuclear modification factor R_{AA} . The leading sources of uncertainty in all muon p_T bins and Pb+Pb collision centralities are the background removal and charm–bottom separation uncertainties, and at low muon p_T in central Pb+Pb collisions the evaluation of the muon efficiency.

6. Results

Fig. 3 shows the differential cross section for muons from charm and bottom hadron decays within $|\eta| < 2$ as a function of muon p_T in pp collisions at $\sqrt{s} = 5.02$ TeV. The measurements are compared with theoretical calculations for muons from D and B meson decays in the FONLL resummation framework [64]. Uncertainties affecting the FONLL calculations include uncertainties in the parton distribution functions, heavy-flavour quark masses, and the renormalization and factorization scales. For muons from charm quarks, the FONLL calculation reaches the experimental data with the upper edge of its uncertainty band at $p_T < 10$ GeV, but underestimates the data at higher p_T . Similar differences between FONLL calculations and prompt-charm measurements were observed in previous measurements at LHC energies, for example, in ALICE measurements of prompt D mesons [65] and inclusive heavy-flavour leptons [16,66], and in an LHCb measurement of prompt D mesons [67]. The measured cross section for muons from bottom quarks is a factor of 1.3–1.4 higher than the FONLL-calculated central value (including $b \rightarrow c \rightarrow \mu$) but still inside the FONLL calculation's uncertainty band at low p_T , while the calculated central value agrees with the data within experimental uncertainties for $p_T > 10$ GeV, similar to observations in a previous ATLAS measurement of non-prompt charmonium [59] and an ALICE measurement of non-prompt D mesons [60].

Fig. 4 shows the differential per-event invariant yields for muons from charm and bottom hadron decays, in Pb+Pb collisions at $\sqrt{s_{NN}} = 5.02$ TeV as a function of muon p_T . To quantify the modification of the momentum distribution between pp and Pb+Pb collisions the nuclear modification factor is calculated according to Eq. (1) in several centrality intervals. The resulting charm and bottom muon R_{AA} values are shown in Fig. 5 as a function of muon p_T . There is substantial suppression of muons from both charm and bottom hadron decays for all analysed Pb+Pb centrality intervals. The suppression increases monotonically from the 40–60% interval to the most central 0–10% interval. The monotonic centrality dependence follows expectations as the heavy quarks spend a longer time in the hotter and larger QGP droplet formed in collisions that have larger nuclear overlap, i.e. the more central inter-

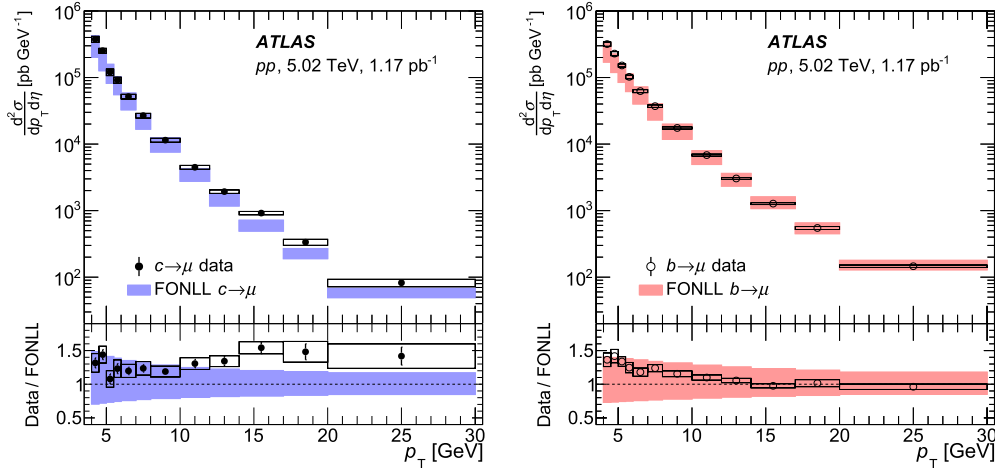


Fig. 3. Differential cross section of charm (left) and bottom (right) muons as a function of muon p_T , plotted at the centres of the p_T intervals, in pp collisions at $\sqrt{s} = 5.02$ TeV in comparison with FONLL calculations. Data results and FONLL calculations for bottom muons both include the $b \rightarrow c \rightarrow \mu$ contribution. Statistical uncertainties in the data are shown as vertical lines and systematic uncertainties in the data and calculation are shown as boxes.

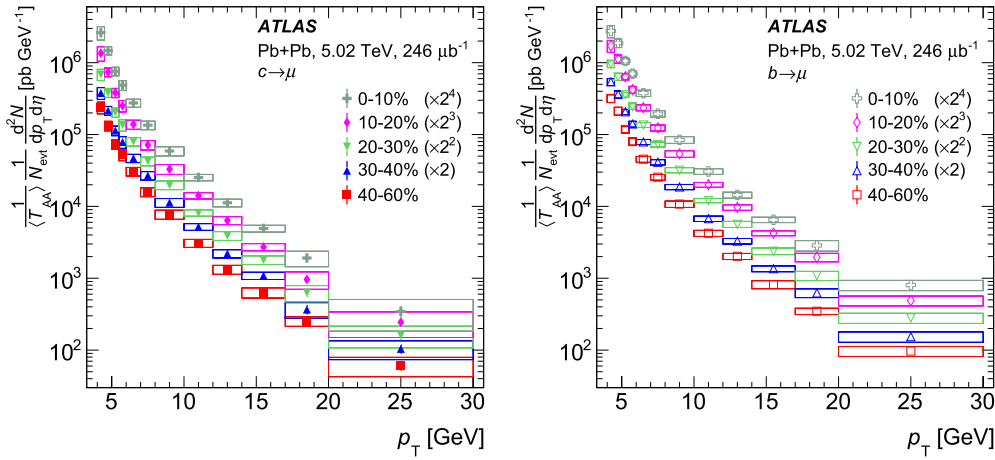


Fig. 4. Differential per-event invariant yields of muons from charm hadron decays (left) and bottom hadron decays (right) as a function of p_T , plotted at the centres of the p_T intervals, for different centrality intervals in Pb+Pb collisions at $\sqrt{s_{NN}} = 5.02$ TeV. For each centrality interval from peripheral to central, an additional scaling factor of 2 is applied to the plotted points for visual clarity. Statistical uncertainties are shown as vertical lines and systematic uncertainties as boxes.

vals. Charm muon R_{AA} shows weak p_T dependence in all centrality intervals, while bottom muon R_{AA} first decreases with increasing muon p_T up to 10 GeV and then remains mostly unchanged in all centralities.

Muons from charm decays have a stronger suppression than muons from bottom decays at low p_T in all centrality intervals. This difference in suppression is highlighted in Fig. 6, which overlays the 0–10% and 40–60% centrality intervals already presented in Fig. 5 for both charm and bottom muon R_{AA} . The mass ordering of the measured R_{AA} follows expectations, as the charm quarks, being lighter than the bottom quarks, are expected to lose more energy in the QGP. Thus the charm quarks are pushed further to lower p_T , and emerge more strongly suppressed than bottom quarks when compared with the cross section in pp collisions. The decay muon p_T spectrum depends on the p_T spectra of various charm and bottom hadrons in pp and Pb+Pb collisions. A portion of the difference found in the charm and bottom muon R_{AA} results could be attributed to the difference between charm and bottom hadron spectra, and thus full model comparisons are necessary.

Fig. 6 also compares the experimental data with theoretical calculations referred to as DREENA-B [68] and DAB-MOD [69,70]. The DREENA-B calculation includes radiative and collisional energy loss

of the heavy quarks traversing the QGP, the latter modelled via a $1 + 1D$ Bjorken expansion [71] with path-length distributions calculated following the procedure described in Ref. [72]. The width of the band corresponding to the DREENA-B theoretical uncertainties reflects the range of the ratio of magnetic to electric screening masses as constrained by non-perturbative calculations [71]. As discussed in Ref. [68], the predicted R_{AA} is higher for B mesons than for D mesons, converging to the same value at $p_T \approx 25$ GeV as is expected when the particle p_T becomes much larger than the mass of the heavier b -quark. The corresponding R_{AA} for muons shown for direct comparison with the experimental data is calculated using PYTHIA8, which simulates meson decay kinematics. The DREENA-B prediction is in reasonable agreement with the experimental data. The DAB-MOD framework used here includes calculations with only Langevin drag and diffusion contributions for the heavy quarks in the QGP. The curves shown here are obtained with TRENTO geometric initial conditions [73], heavy-quark Langevin dynamics with the Moore and Teaney parameterization [74], and coupling values for charm (bottom) of $D/2\pi T = 2.23$ (2.79), where D is the spatial diffusion coefficient and T is the temperature. The temperature at which heavy quarks decouple from the medium is $T = 160$ MeV and both coalescence and fragmentation are implemented for hadronization. The DAB-MOD predictions with only

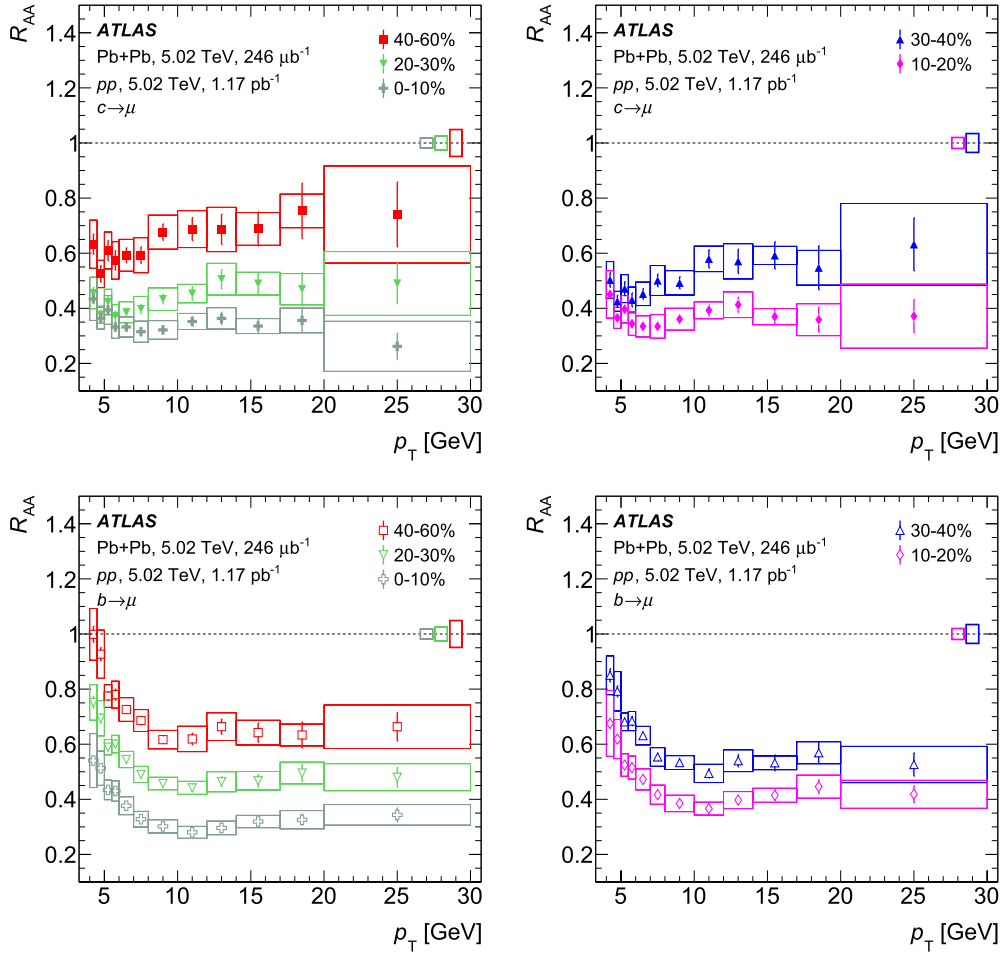


Fig. 5. Nuclear modification factor, R_{AA} , for muons from charm hadron decays (top panels) and bottom hadron decays (bottom panels) as a function of p_T for five different centrality intervals. The centrality intervals are separated for clarity into the left (0–10%, 20–30%, 40–60%) and right (10–20%, 30–40%) panels. Statistical uncertainties are shown as vertical lines and uncorrelated systematic uncertainties as boxes around the points. Correlated fractional systematic uncertainties, including T_{AA} and pp luminosity uncertainties, are isolated as coloured boxes around unity for different centrality intervals.

Langevin dynamics shown in Fig. 6 as coloured solid lines are in qualitative agreement with the experimental data, but have a stronger p_T dependence than the experimental data, particularly in the most central collisions. No uncertainties are included for DAB-MOD calculations shown here.

It is notable that both of these calculations also predict the azimuthal anisotropies of the heavy-flavour muons. ATLAS has previously published azimuthal anisotropies quantified by the elliptic flow coefficient, v_2 , for muons from charm and bottom hadron decays [25]. The lower panels of Fig. 6 show those ATLAS measurements of v_2 as a function of p_T in comparison with both the DREENA-B and DAB-MOD calculations. The DREENA-B calculations agree qualitatively with both v_2 and R_{AA} for both charm and bottom muons, while the previously described implementation of DAB-MOD underestimates the charm muon v_2 even though it qualitatively matches the R_{AA} . In all theoretical implementations, a larger coupling of charm and bottom quarks to the QGP results in a reduced R_{AA} (i.e. more suppression) and an increased v_2 (i.e. larger anisotropy). Thus, increasing the coupling of charm to the QGP in DAB-MOD, for example, could bring the predicted v_2 into closer agreement with data but would simultaneously decrease R_{AA} , pushing the calculation further below the data. That said, another key component of these calculations is the modelling of the QGP space-time evolution, and thus it could be instructive in the future to compare the different theory calculations with a common QGP model to test whether the differences in R_{AA} and

v_2 arise from the QGP modelling or the energy-loss implementation.

Fig. 7 shows the measured ratio of charm muon R_{AA} to bottom muon R_{AA} as a function of p_T in comparison with DREENA-B and DAB-MOD calculations. The large uncertainty in the measured ratio is due to a strong negative correlation between the charm and bottom muon R_{AA} uncertainties. As indicated by the measured R_{AA} ratios, charm muons are significantly more suppressed than bottom muons in the $p_T < 8$ GeV range. However, no strong conclusion about the relative strength of their suppression can be drawn at higher p_T with existing large uncertainties. Compared with the ratios measured in data, the calculations underestimate the R_{AA} ratios for 0–10% centrality, while they mostly capture the magnitude and p_T dependence of the ratio for 40–60% centrality. As shown in Fig. 6, the discrepancy between data and the models in the 0–10% centrality interval is primarily due to the underestimation of charm muon R_{AA} .

7. Conclusion

The ATLAS experiment at the LHC has measured the production rates and nuclear modification factors, R_{AA} , of muons from semileptonic decays of heavy-flavour hadrons in pp and Pb+Pb collisions at 5.02 TeV. The measurement uses 2017 pp data and combined 2015 and 2018 Pb+Pb data corresponding to integrated luminosities of 1.17 pb^{-1} and 246 μb^{-1} respectively. Compared to

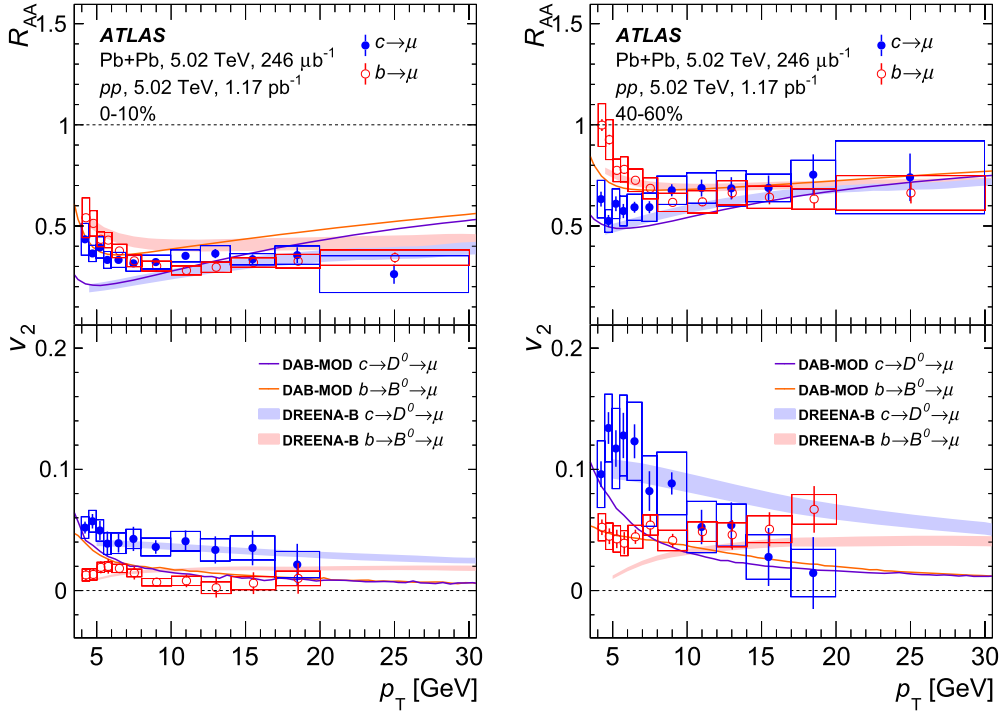


Fig. 6. Nuclear modification factor, R_{AA} , (top) and elliptic flow, v_2 , results taken from Ref. [25] (bottom) for muons from bottom hadron decays and charm hadron decays for 0–10% (left) and 40–60% (right) centrality intervals as a function of p_T . Statistical uncertainties are shown as vertical lines and systematic uncertainties as boxes. Also shown are theoretical calculations from the DREENA-B and DAB-MOD models. See text regarding the uncertainty band of DREENA-B model calculations.

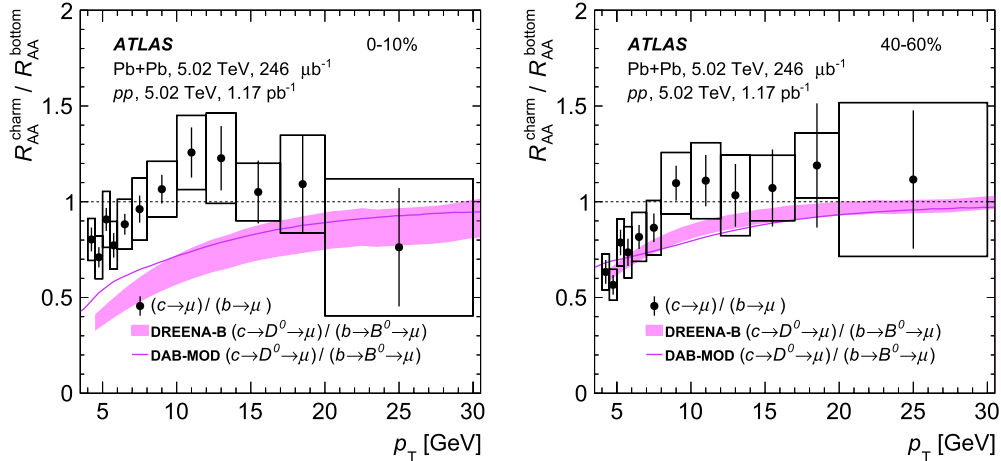


Fig. 7. The ratio of charm muon R_{AA} to bottom muon R_{AA} , $R_{AA}^{\text{charm}}/R_{AA}^{\text{bottom}}$, for 0–10% (left) and 40–60% (right) Pb+Pb centrality intervals as a function of muon p_T . Statistical uncertainties are shown as vertical lines and systematic uncertainties as boxes. Also shown are theoretical calculations for the decay muons from DREENA-B and DAB-MOD in the same centrality intervals.

a previous ATLAS measurement of heavy-flavour muons, this Letter reports separate results for charm and bottom muons and covers a wider p_T range. The differential cross section measured in pp collisions for muons from decays of hadrons containing a bottom quark is reproduced with FONLL calculations. For muons from decays of hadrons containing a charm quark, the FONLL calculation is lower than the data at all measured p_T but agrees with it within the systematic uncertainties of the calculations below 10 GeV. The R_{AA} measurements indicate a significant suppression of the yield of muons from both charm and bottom hadron decays, with a suppression that increases monotonically from peripheral to central collisions.

The suppression is stronger for charm quarks than for bottom quarks, as seen via muons at low $p_T < 10$ GeV. The relative dif-

ference between charm and bottom suppression is consistent with theoretical expectations for 10–60% Pb+Pb collisions, while the difference is smaller in data compared to theory for 0–10% Pb+Pb collisions. The simultaneous constraints imposed by the measurements of R_{AA} presented here and the flow measurements previously published by ATLAS could provide important information for understanding heavy-quark transport and QGP properties.

Declaration of competing interest

The authors declare that they have no known competing financial interests or personal relationships that could have appeared to influence the work reported in this paper.

Acknowledgements

We thank CERN for the very successful operation of the LHC, as well as the support staff from our institutions without whom ATLAS could not be operated efficiently.

We acknowledge the support of ANPCyT, Argentina; YerPhI, Armenia; ARC, Australia; BMWFW and FWF, Austria; ANAS, Azerbaijan; SSTC, Belarus; CNPq and FAPESP, Brazil; NSERC, NRC and CFI, Canada; CERN; ANID, Chile; CAS, MOST and NSFC, China; Minciencias, Colombia; MEYS CR, Czech Republic; DNRF and DNSRC, Denmark; IN2P3-CNRS and CEA-DRF/IRFU, France; SRNSFG, Georgia; BMBF, HGF and MPG, Germany; GSRI, Greece; RGC and Hong Kong SAR, China; ISF and Benozio Center, Israel; INFN, Italy; MEXT and JSPS, Japan; CNRST, Morocco; NWO, Netherlands; RCN, Norway; MEiN, Poland; FCT, Portugal; MNE/IFA, Romania; JINR; MES of Russia and NRC KI, Russian Federation; MESTD, Serbia; MSSR, Slovakia; ARRS and MIZŠ, Slovenia; DSI/NRF, South Africa; MICINN, Spain; SRC and Wallenberg Foundation, Sweden; SERI, SNSF and Cantons of Bern and Geneva, Switzerland; MOST, Taiwan; TAEK, Turkey; STFC, United Kingdom; DOE and NSF, United States of America. In addition, individual groups and members have received support from BCKDF, CANARIE, Compute Canada and CRC, Canada; COST, ERC, ERDF, Horizon 2020 and Marie Skłodowska-Curie Actions, European Union; Investissements d'Avenir Labex, Investissements d'Avenir Idex and ANR, France; DFG and AvH Foundation, Germany; Herakleitos, Thales and Aristeia programmes co-financed by EU-ESF and the Greek NSRF, Greece; BSF-NSF and GIF, Israel; Norwegian Financial Mechanism 2014-2021, Norway; NCN and NAWA, Poland; La Caixa Banking Foundation, CERCA Programme Generalitat de Catalunya and PROMETEO and GenT Programmes Generalitat Valenciana, Spain; Göran Gustafssons Stiftelser, Sweden; The Royal Society and Leverhulme Trust, United Kingdom.

The crucial computing support from all WLCG partners is acknowledged gratefully, in particular from CERN, the ATLAS Tier-1 facilities at TRIUMF (Canada), NDGF (Denmark, Norway, Sweden), CC-IN2P3 (France), KIT/GridKA (Germany), INFN-CNAF (Italy), NL-T1 (Netherlands), PIC (Spain), ASGC (Taiwan), RAL (UK) and BNL (USA), the Tier-2 facilities worldwide and large non-WLCG resource providers. Major contributors of computing resources are listed in Ref. [75].

References

- [1] U. Heinz, R. Snellings, Collective flow and viscosity in relativistic heavy-ion collisions, *Annu. Rev. Nucl. Part. Sci.* 63 (2013) 123, arXiv:1301.2826 [nucl-th].
- [2] P. Romatschke, U. Romatschke, *Relativistic Fluid Dynamics In and Out of Equilibrium*, Cambridge Monographs on Mathematical Physics, Cambridge University Press, 2019, arXiv:1712.05815 [nucl-th].
- [3] S. Cao, et al., Toward the determination of heavy-quark transport coefficients in quark-gluon plasma, *Phys. Rev. C* 99 (2019) 054907, arXiv:1809.07894 [nucl-th].
- [4] M. Younus, C.E. Coleman-Smith, S.A. Bass, D.K. Srivastava, Charm quark energy loss in infinite QCD matter using a parton cascade model, *Phys. Rev. C* 91 (2015) 024912, arXiv:1309.1276 [nucl-th].
- [5] C.E. Coleman-Smith, B. Muller, Constituent mass dependence of transport coefficients in a quark-gluon plasma, arXiv:1209.3328 [hep-ph], 2012.
- [6] Y.L. Dokshitzer, D.E. Kharzeev, Heavy-quark colorimetry of QCD matter, *Phys. Lett. B* 519 (2001) 199, arXiv:hep-ph/0106202 [hep-ph].
- [7] M. Harrison, S. Peggs, T. Roser, The RHIC accelerator, *Annu. Rev. Nucl. Part. Sci.* 52 (2002) 425.
- [8] L. Evans, P. Bryant, LHC machine, *J. Instrum.* 3 (2008) S08001.
- [9] X. Dong, Y.-J. Lee, R. Rapp, Open heavy-flavor production in heavy-ion collisions, *Annu. Rev. Nucl. Part. Sci.* 69 (2019) 417, arXiv:1903.07709 [nucl-ex].
- [10] R. Averbeck, Heavy-flavor production in heavy-ion collisions and implications for the properties of hot QCD matter, *Prog. Part. Nucl. Phys.* 70 (2013) 159, arXiv:1505.03828 [nucl-ex].
- [11] M.L. Miller, K. Reygers, S.J. Sanders, P. Steinberg, Glauber modeling in high-energy nuclear collisions, *Annu. Rev. Nucl. Part. Sci.* 57 (2007) 205, arXiv:nucl-ex/0701025 [nucl-ex].
- [12] ATLAS Collaboration, Measurement of the suppression and azimuthal anisotropy of muons from heavy-flavor decays in Pb+Pb collisions at $\sqrt{s_{NN}} = 2.76$ TeV with the ATLAS detector, *Phys. Rev. C* 98 (2018) 044905, arXiv:1805.05220 [hep-ex].
- [13] ALICE Collaboration, Production of muons from heavy-flavour hadron decays at high transverse momentum in Pb-Pb collisions at $\sqrt{s_{NN}} = 5.02$ and 2.76 TeV, *Phys. Lett. B* 820 (2021) 136558, arXiv:2011.05718 [nucl-ex].
- [14] ALICE Collaboration, Measurements of low- p_T electrons from semileptonic heavy-flavour hadron decays at mid-rapidity in pp and Pb-Pb collisions at $\sqrt{s_{NN}} = 2.76$ TeV, *J. High Energy Phys.* 10 (2018) 061, arXiv:1805.04379 [nucl-ex].
- [15] ALICE Collaboration, Measurement of the production of high- p_T electrons from heavy-flavour hadron decays in Pb-Pb collisions at $\sqrt{s_{NN}} = 2.76$ TeV, *Phys. Lett. B* 771 (2017) 467, arXiv:1609.07104 [nucl-ex].
- [16] ALICE Collaboration, Measurement of electrons from semileptonic heavy-flavour hadron decays at midrapidity in pp and Pb-Pb collisions at $\sqrt{s_{NN}} = 5.02$ TeV, *Phys. Lett. B* 804 (2020) 135377, arXiv:1910.09110 [nucl-ex].
- [17] CMS Collaboration, Nuclear modification factor of D^0 mesons in PbPb collisions at $\sqrt{s_{NN}} = 5.02$ TeV, *Phys. Lett. B* 782 (2018) 474, arXiv:1708.04962 [hep-ex].
- [18] ALICE Collaboration, Measurement of D^0 , D^+ , D^{*+} and D_s^+ production in Pb-Pb collisions at $\sqrt{s_{NN}} = 5.02$ TeV, *J. High Energy Phys.* 10 (2018) 174, arXiv:1804.09083 [nucl-ex].
- [19] ALICE Collaboration, Λ_c^+ production in Pb-Pb collisions at $\sqrt{s_{NN}} = 5.02$ TeV, *Phys. Lett. B* 793 (2019) 212, arXiv:1809.10922 [nucl-ex].
- [20] STAR Collaboration, J. Adam, et al., Centrality and transverse momentum dependence of D^0 -meson production at mid-rapidity in Au+Au collisions at $\sqrt{s_{NN}} = 200$ GeV, *Phys. Rev. C* 99 (2019) 034908, arXiv:1812.10224 [nucl-ex].
- [21] STAR Collaboration, L. Adamczyk, et al., Observation of D^0 meson nuclear modifications in Au+Au collisions at $\sqrt{s_{NN}} = 200$ GeV, *Phys. Rev. Lett.* 113 (2014) 142301, arXiv:1404.6185 [nucl-ex]; Erratum: *Phys. Rev. Lett.* 121 (2018) 229901.
- [22] STAR Collaboration, J. Adam, et al., Observation of D_s^\pm/D^0 enhancement in Au+Au collisions at $\sqrt{s_{NN}} = 200$ GeV, arXiv:2101.11793 [hep-ex], 2021.
- [23] STAR Collaboration, J. Adam, et al., First measurement of Λ_c baryon production in Au+Au collisions at $\sqrt{s_{NN}} = 200$ GeV, *Phys. Rev. Lett.* 124 (2020) 172301, arXiv:1910.14628 [nucl-ex].
- [24] ATLAS Collaboration, Measurement of azimuthal anisotropy of muons from charm and bottom hadrons in pp collisions at $\sqrt{s} = 13$ TeV with the ATLAS detector, *Phys. Rev. Lett.* 124 (2020) 082301, arXiv:1909.01650 [hep-ex].
- [25] ATLAS Collaboration, Measurement of azimuthal anisotropy of muons from charm and bottom hadrons in Pb+Pb collisions at $\sqrt{s_{NN}} = 5.02$ TeV with the ATLAS detector, *Phys. Lett. B* 807 (2020) 135595, arXiv:2003.03565 [hep-ex].
- [26] ATLAS Collaboration, The ATLAS experiment at the CERN large hadron collider, *J. Instrum.* 3 (2008) S08003.
- [27] ATLAS Collaboration, ATLAS insertable B-layer technical design report, ATLAS-TDR-19; CERN-LHCC-2010-013, <https://cds.cern.ch/record/1291633>, 2010; Addendum: ATLAS-TDR-19-ADD-1; CERN-LHCC-2012-009, <https://cds.cern.ch/record/1451888>, 2012.
- [28] B. Abbott, et al., Production and integration of the ATLAS insertable B-layer, *J. Instrum.* 13 (2018) T05008, arXiv:1803.00844 [physics.ins-det].
- [29] ATLAS Collaboration, Performance of the ATLAS trigger system in 2015, *Eur. Phys. J. C* 77 (2017) 317, arXiv:1611.09661 [hep-ex].
- [30] ATLAS Collaboration, The ATLAS collaboration software and firmware, ATLSOFT-PUB-2021-001, <https://cds.cern.ch/record/2767187>, 2021.
- [31] ATLAS Collaboration, Performance of the ATLAS muon triggers in Run 2, *J. Instrum.* 15 (2020) P09015, arXiv:2004.13447 [hep-ex].
- [32] J.P. Guillaud, A.E. Sobol, Simulation of diffractive and non-diffractive processes at the LHC energy with the PYTHIA and PHOJET MC event generators, *Tech. Rep.*, 2004, <http://hal.in2p3.fr/in2p3-00021835>.
- [33] ATLAS Collaboration, Measurement of the azimuthal anisotropy of charged particles produced in $\sqrt{s_{NN}} = 5.02$ TeV Pb+Pb collisions with the ATLAS detector, *Eur. Phys. J. C* 78 (2018) 997, arXiv:1808.03951 [hep-ex].
- [34] ATLAS Collaboration, Muon reconstruction performance of the ATLAS detector in proton-proton collision data at $\sqrt{s} = 13$ TeV, *Eur. Phys. J. C* 76 (2016) 292, arXiv:1603.05598 [hep-ex].
- [35] T. Sjöstrand, et al., An introduction to PYTHIA 8.2, *Comput. Phys. Commun.* 191 (2015) 159, arXiv:1410.3012 [hep-ph].
- [36] S. Agostinelli, et al., GEANT4 — a simulation toolkit, *Nucl. Instrum. Methods A* 506 (2003) 250.
- [37] ATLAS Collaboration, The ATLAS simulation infrastructure, *Eur. Phys. J. C* 70 (2010) 823, arXiv:1005.4568 [physics.ins-det].
- [38] ATLAS Collaboration, Measurements of the electron and muon inclusive cross-sections in proton-proton collisions at $\sqrt{s} = 7$ TeV with the ATLAS detector, *Phys. Lett. B* 707 (2012) 438, arXiv:1109.0525 [hep-ex].
- [39] ATLAS Collaboration, Measurements of W and Z boson production in pp collisions at $\sqrt{s} = 5.02$ TeV with the ATLAS detector, *Eur. Phys. J. C* 79 (2019) 128, arXiv:1810.08424 [hep-ex]; Erratum: *Eur. Phys. J. C* 79 (2019) 374.
- [40] ATLAS Collaboration, Measurement of W^\pm boson production in Pb+Pb collisions at $\sqrt{s_{NN}} = 5.02$ TeV with the ATLAS detector, *Eur. Phys. J. C* 79 (2019) 935, arXiv:1907.10414 [hep-ex].

- [41] G.T. Bodwin, E. Braaten, G.P. Lepage, Rigorous QCD analysis of inclusive annihilation and production of heavy quarkonium, *Phys. Rev. D* 51 (1995) 1125, arXiv:hep-ph/9407339 [hep-ph]; Erratum: *Phys. Rev. D* 55 (1997) 5853.
- [42] S. Alioli, P. Nason, C. Oleari, E. Re, A general framework for implementing NLO calculations in shower Monte Carlo programs: the POWHEG BOX, *J. High Energy Phys.* 06 (2010) 043, arXiv:1002.2581 [hep-ph].
- [43] H.-L. Lai, et al., New parton distributions for collider physics, *Phys. Rev. D* 82 (2010) 074024, arXiv:1007.2241 [hep-ph].
- [44] J. Pumplin, et al., New generation of parton distributions with uncertainties from global QCD analysis, *J. High Energy Phys.* 07 (2002) 012, arXiv:hep-ph/0201195.
- [45] ATLAS Collaboration, Measurement of quarkonium production in proton-lead and proton-proton collisions at 5.02 TeV with the ATLAS detector, *Eur. Phys. J. C* 78 (2018) 171, arXiv:1709.03089 [hep-ex].
- [46] ATLAS Collaboration, Prompt and non-prompt J/ψ and $\psi(2S)$ suppression at high transverse momentum in 5.02 TeV Pb+Pb collisions with the ATLAS experiment, *Eur. Phys. J. C* 78 (2018) 762, arXiv:1805.04077 [hep-ex].
- [47] CMS Collaboration, Measurement of nuclear modification factors of $\Upsilon(1S)$, $\Upsilon(2S)$, and $\Upsilon(3S)$ mesons in PbPb collisions at $\sqrt{s_{NN}} = 5.02$ TeV, *Phys. Lett. B* 790 (2019) 270, arXiv:1805.09215 [hep-ex].
- [48] ATLAS Collaboration, Z boson production in Pb+Pb collisions at $\sqrt{s_{NN}} = 5.02$ TeV measured by the ATLAS experiment, *Phys. Lett. B* 802 (2020) 135262, arXiv:1910.13396 [hep-ex].
- [49] ATLAS Collaboration, ATLAS Pythia 8 tunes to 7 TeV data, ATL-PHYS-PUB-2014-021, <https://cds.cern.ch/record/1966419>, 2014.
- [50] R.D. Ball, et al., Parton distributions with LHC data, *Nucl. Phys. B* 867 (2013) 244, arXiv:1207.1303 [hep-ph].
- [51] ATLAS Collaboration, Reconstruction of primary vertices at the ATLAS experiment in Run 1 proton-proton collisions at the LHC, *Eur. Phys. J. C* 77 (2017) 332, arXiv:1611.10235 [hep-ex].
- [52] M. Cacciari, M. Greco, P. Nason, The p_T spectrum in heavy-flavour hadroproduction, *J. High Energy Phys.* 05 (1998) 007, arXiv:hep-ph/9803400 [hep-ph].
- [53] M. Cacciari, S. Frixione, P. Nason, The p_T spectrum in heavy-flavour photoproduction, *J. High Energy Phys.* 03 (2001) 006, arXiv:hep-ph/0102134 [hep-ph].
- [54] M. Lisovsky, A. Verbitskiy, O. Zenaiev, Combined analysis of charm-quark fragmentation-fraction measurements, *Eur. Phys. J. C* 76 (2016) 397, arXiv:1509.01061 [hep-ex].
- [55] CDF Collaboration, T. Aaltonen, et al., Measurement of ratios of fragmentation fractions for bottom hadrons in $p\bar{p}$ collisions at $\sqrt{s} = 1.96$ TeV, *Phys. Rev. C* 77 (2008) 072003, arXiv:0801.4375 [hep-ex].
- [56] A.M. Sirunyan, et al., Production of Λ_c^+ baryons in proton-proton and lead-lead collisions at $\sqrt{s_{NN}} = 5.02$ TeV, *Phys. Lett. B* 803 (2020) 135328, arXiv:1906.03322 [hep-ex].
- [57] Particle Data Group, P.A. Zyla, et al., Review of particle physics, *Prog. Theor. Exp. Phys.* 2020 (2020) 083C01.
- [58] E. Lohrmann, A summary of charm hadron production fractions, arXiv:1112.3757 [hep-ex], 2011.
- [59] ATLAS Collaboration, Measurement of the differential cross-sections of prompt and non-prompt production of J/ψ and $\psi(2S)$ in pp collisions at $\sqrt{s} = 7$ and 8 TeV with the ATLAS detector, *Eur. Phys. J. C* 76 (2016) 283, arXiv:1512.03657 [hep-ex].
- [60] ALICE Collaboration, Measurement of beauty and charm production in pp collisions at $\sqrt{s} = 5.02$ TeV via non-prompt and prompt D mesons, *J. High Energy Phys.* 05 (2021) 220, arXiv:2102.13601 [nucl-ex].
- [61] ALICE Collaboration, Measurement of charm production at central rapidity in proton-proton collisions at $\sqrt{s} = 7$ TeV, *J. High Energy Phys.* 01 (2012) 128, arXiv:1111.1553 [hep-ex].
- [62] G. Avoni, et al., The new LUCID-2 detector for luminosity measurement and monitoring in ATLAS, *J. Instrum.* 13 (2018) P07017.
- [63] ATLAS Collaboration, Luminosity determination in pp collisions at $\sqrt{s} = 13$ TeV using the ATLAS detector at the LHC, ATLAS-CONF-2019-021, <https://cds.cern.ch/record/2677054>, 2019.
- [64] M. Cacciari, et al., Theoretical predictions for charm and bottom production at the LHC, *J. High Energy Phys.* 10 (2012) 137, arXiv:1205.6344 [hep-ph].
- [65] ALICE Collaboration, Measurement of D^0 , D^+ , D^{*+} and D_s^+ production in pp collisions at $\sqrt{s} = 5.02$ TeV with ALICE, *Eur. Phys. J. C* 79 (2019) 388, arXiv:1901.07979 [nucl-ex].
- [66] ALICE Collaboration, Production of muons from heavy-flavour hadron decays in pp collisions at $\sqrt{s} = 5.02$ TeV, *J. High Energy Phys.* 09 (2019) 008, arXiv:1905.07207 [nucl-ex].
- [67] LHCb Collaboration, Measurements of prompt charm production cross-sections in pp collisions at $\sqrt{s} = 5$ TeV, *J. High Energy Phys.* 06 (2017) 147, arXiv:1610.02230 [hep-ex].
- [68] D. Zigic, I. Salom, J. Auvinen, M. Djordjevic, M. Djordjevic, DREENA-B framework: first predictions of R_{AA} and v_2 within dynamical energy loss formalism in evolving QCD medium, *Phys. Lett. B* 791 (2019) 236, arXiv:1805.04786 [nucl-th].
- [69] R. Katz, C.A.G. Prado, J. Noronha-Hostler, J. Noronha, A.A.P. Suaide, Sensitivity study with a D and B mesons modular simulation code of heavy flavor R_{AA} and azimuthal anisotropies based on beam energy, initial conditions, hadronization, and suppression mechanisms, *Phys. Rev. C* 102 (2020) 024906, arXiv:1906.10768 [nucl-th].
- [70] C.A.G. Prado, et al., Event-by-event correlations between soft hadrons and D^0 mesons in 5.02 TeV PbPb collisions at the CERN Large Hadron Collider, *Phys. Rev. C* 96 (2017) 064903, arXiv:1611.02965 [nucl-th].
- [71] J.D. Bjorken, Highly relativistic nucleus-nucleus collisions: the central rapidity region, *Phys. Rev. D* 27 (1983) 140.
- [72] A. Dainese, Perspectives for the study of charm in-medium quenching at the LHC with ALICE, *Eur. Phys. J. C* 33 (2004) 495, arXiv:nucl-ex/0312005.
- [73] J.S. Moreland, J.E. Bernhard, S.A. Bass, Alternative ansatz to wounded nucleon and binary collision scaling in high-energy nuclear collisions, *Phys. Rev. C* 92 (2015) 011901, arXiv:1412.4708 [nucl-th].
- [74] G.D. Moore, D. Teaney, How much do heavy quarks thermalize in a heavy ion collision?, *Phys. Rev. C* 71 (2005) 064904, arXiv:hep-ph/0412346 [hep-ph].
- [75] ATLAS Collaboration, ATLAS computing acknowledgements, ATL-SOFT-PUB-2021-003, <https://cds.cern.ch/record/2776662>.

The ATLAS Collaboration

G. Aad⁹⁹, B. Abbott¹²⁴, D.C. Abbott¹⁰⁰, A. Abed Abud³⁴, K. Abeling⁵¹, D.K. Abhayasinghe⁹¹, S.H. Abidi²⁷, H. Abramowicz¹⁵⁷, H. Abreu¹⁵⁶, Y. Abulaiti⁵, A.C. Abusleme Hoffman^{142a}, B.S. Acharya^{64a,64b,p}, B. Achkar⁵¹, L. Adam⁹⁷, C. Adam Bourdarios⁴, L. Adamczyk^{81a}, L. Adamek¹⁶², S.V. Addepalli²⁴, J. Adelman¹¹⁷, A. Adiguzel^{11c,ae}, S. Adorni⁵², T. Adye¹³⁹, A.A. Affolder¹⁴¹, Y. Afik¹⁵⁶, C. Agapopoulou⁶², M.N. Agaras¹², J. Agarwala^{68a,68b}, A. Aggarwal¹¹⁵, C. Agheorghiesei^{25c}, J.A. Aguilar-Saavedra^{135f,135a,ad}, A. Ahmad³⁴, F. Ahmadov⁷⁷, W.S. Ahmed¹⁰¹, X. Ai⁴⁴, G. Aielli^{71a,71b}, I. Aizenberg¹⁷⁵, S. Akatsuka⁸³, M. Akbiyik⁹⁷, T.P.A. Åkesson⁹⁴, A.V. Akimov¹⁰⁸, K. Al Khoury³⁷, G.L. Alberghi^{21b}, J. Albert¹⁷¹, P. Albicocco⁴⁹, M.J. Alconada Verzini⁸⁶, S. Alderweireldt⁴⁸, M. Aleksa³⁴, I.N. Aleksandrov⁷⁷, C. Alexa^{25b}, T. Alexopoulos⁹, A. Alfonsi¹¹⁶, F. Alfonsi^{21b}, M. Alhroob¹²⁴, B. Ali¹³⁷, S. Ali¹⁵⁴, M. Aliev¹⁶¹, G. Alimonti^{66a}, C. Allaire³⁴, B.M.M. Allbrooke¹⁵², P.P. Allport¹⁹, A. Aloisio^{67a,67b}, F. Alonso⁸⁶, C. Alpigiani¹⁴⁴, E. Alunno Camelia^{71a,71b}, M. Alvarez Estevez⁹⁶, M.G. Alviggi^{67a,67b}, Y. Amaral Coutinho^{78b}, A. Ambler¹⁰¹, L. Ambroz¹³⁰, C. Amelung³⁴, D. Amidei¹⁰³, S.P. Amor Dos Santos^{135a}, S. Amoroso⁴⁴, C.S. Amrouche⁵², C. Anastopoulos¹⁴⁵, N. Andari¹⁴⁰, T. Andeen¹⁰, J.K. Anders¹⁸, S.Y. Andrean^{43a,43b}, A. Andreazza^{66a,66b}, S. Angelidakis⁸, A. Angerami³⁷, A.V. Anisenkov^{118b,118a}, A. Annovi^{69a}, C. Antel⁵², M.T. Anthony¹⁴⁵, E. Antipov¹²⁵, M. Antonelli⁴⁹, D.J.A. Antrim¹⁶, F. Anulli^{70a}, M. Aoki⁷⁹, J.A. Aparisi Pozo¹⁶⁹, M.A. Aparo¹⁵², L. Aperio Bella⁴⁴, N. Aranzabal³⁴, V. Araujo Ferraz^{78a}, C. Arcangeletti⁴⁹, A.T.H. Arce⁴⁷, E. Arena⁸⁸, J-F. Arguin¹⁰⁷, S. Argyropoulos⁵⁰, J.-H. Arling⁴⁴, A.J. Armbruster³⁴, A. Armstrong¹⁶⁶, O. Arnaez¹⁶², H. Arnold³⁴,

Z.P. Arrubarrena Tame¹¹¹, G. Artoni¹³⁰, H. Asada¹¹³, K. Asai¹²², S. Asai¹⁵⁹, N.A. Asbah⁵⁷, E.M. Asimakopoulou¹⁶⁷, L. Asquith¹⁵², J. Assahsah^{33d}, K. Assamagan²⁷, R. Astalos^{26a}, R.J. Atkin^{31a}, M. Atkinson¹⁶⁸, N.B. Atlay¹⁷, H. Atmani^{58b}, P.A. Atlasiddha¹⁰³, K. Augsten¹³⁷, S. Auricchio^{67a,67b}, V.A. Austrup¹⁷⁷, G. Avner¹⁵⁶, G. Avolio³⁴, M.K. Ayoub^{13c}, G. Azuelos^{107,al}, D. Babal^{26a}, H. Bachacou¹⁴⁰, K. Bachas¹⁵⁸, A. Bachiu³², F. Backman^{43a,43b}, A. Badea⁵⁷, P. Bagnaia^{70a,70b}, H. Bahrasemani¹⁴⁸, A.J. Bailey¹⁶⁹, V.R. Bailey¹⁶⁸, J.T. Baines¹³⁹, C. Bakalis⁹, O.K. Baker¹⁷⁸, P.J. Bakker¹¹⁶, E. Bakos¹⁴, D. Bakshi Gupta⁷, S. Balaji¹⁵³, R. Balasubramanian¹¹⁶, E.M. Baldin^{118b,118a}, P. Balek¹³⁸, E. Ballabene^{66a,66b}, F. Balli¹⁴⁰, W.K. Balunas¹³⁰, J. Balz⁹⁷, E. Banas⁸², M. Bandieramonte¹³⁴, A. Bandyopadhyay¹⁷, S. Bansal²², L. Barak¹⁵⁷, E.L. Barberio¹⁰², D. Barberis^{53b,53a}, M. Barbero⁹⁹, G. Barbour⁹², K.N. Barends^{31a}, T. Barillari¹¹², M-S. Barisits³⁴, J. Barkeloo¹²⁷, T. Barklow¹⁴⁹, B.M. Barnett¹³⁹, R.M. Barnett¹⁶, A. Baroncelli^{58a}, G. Barone²⁷, A.J. Barr¹³⁰, L. Barranco Navarro^{43a,43b}, F. Barreiro⁹⁶, J. Barreiro Guimarães da Costa^{13a}, U. Barron¹⁵⁷, S. Barsov¹³³, F. Bartels^{59a}, R. Bartoldus¹⁴⁹, G. Bartolini⁹⁹, A.E. Barton⁸⁷, P. Bartos^{26a}, A. Basalae⁴⁴, A. Basan⁹⁷, I. Bashta^{72a,72b}, A. Bassalat^{62,ai}, M.J. Basso¹⁶², C.R. Basson⁹⁸, R.L. Bates⁵⁵, S. Batlamous^{33e}, J.R. Batley³⁰, B. Batool¹⁴⁷, M. Battaglia¹⁴¹, M. Bause^{70a,70b}, F. Bauer^{140,*}, P. Bauer²², H.S. Bawa²⁹, A. Bayirli^{11c}, J.B. Beacham⁴⁷, T. Beau¹³¹, P.H. Beauchemin¹⁶⁵, F. Becherer⁵⁰, P. Bechtel²², H.P. Beck^{18,r}, K. Becker¹⁷³, C. Becot⁴⁴, A.J. Beddall^{11a}, V.A. Bednyakov⁷⁷, C.P. Bee¹⁵¹, T.A. Beermann¹⁷⁷, M. Begalli^{78b}, M. Begel²⁷, A. Behera¹⁵¹, J.K. Behr⁴⁴, C. Beirao Da Cruz E Silva³⁴, J.F. Beirer^{51,34}, F. Beisiegel²², M. Belfkir⁴, G. Bella¹⁵⁷, L. Bellagamba^{21b}, A. Bellerive³², P. Bellos¹⁹, K. Beloborodov^{118b,118a}, K. Belotskiy¹⁰⁹, N.L. Belyaev¹⁰⁹, D. Benckekroun^{33a}, Y. Benhammou¹⁵⁷, D.P. Benjamin²⁷, M. Benoit²⁷, J.R. Bensinger²⁴, S. Bentvelsen¹¹⁶, L. Beresford³⁴, M. Beretta⁴⁹, D. Berge¹⁷, E. Bergeaas Kuutmann¹⁶⁷, N. Berger⁴, B. Bergmann¹³⁷, L.J. Bergsten²⁴, J. Beringer¹⁶, S. Berlendis⁶, G. Bernardi¹³¹, C. Bernius¹⁴⁹, F.U. Bernlochner²², T. Berry⁹¹, P. Berta¹³⁸, A. Berthold⁴⁶, I.A. Bertram⁸⁷, O. Bessidskaia Bylund¹⁷⁷, S. Bethke¹¹², A. Betti⁴⁰, A.J. Bevan⁹⁰, S. Bhatta¹⁵¹, D.S. Bhattacharya¹⁷², P. Bhattarai²⁴, V.S. Bhopatkar⁵, R. Bi¹³⁴, R.M. Bianchi¹³⁴, O. Biebel¹¹¹, R. Bielski¹²⁷, N.V. Biesuz^{69a,69b}, M. Biglietti^{72a}, T.R.V. Billoud¹³⁷, M. Bindi⁵¹, A. Bingul^{11d}, C. Bini^{70a,70b}, S. Biondi^{21b,21a}, A. Biondini⁸⁸, C.J. Birch-sykes⁹⁸, G.A. Bird^{19,139}, M. Birman¹⁷⁵, T. Bisanz³⁴, J.P. Biswal², D. Biswas^{176,k}, A. Bitadze⁹⁸, C. Bittrich⁴⁶, K. Bjørke¹²⁹, I. Bloch⁴⁴, C. Blocker²⁴, A. Blue⁵⁵, U. Blumenschein⁹⁰, J. Blumenthal⁹⁷, G.J. Bobbink¹¹⁶, V.S. Bobrovnikov^{118b,118a}, M. Boehler⁵⁰, D. Bogavac¹², A.G. Bogdanchikov^{118b,118a}, C. Boehm^{43a}, V. Boisvert⁹¹, P. Bokan⁴⁴, T. Bold^{81a}, M. Bomben¹³¹, M. Bona⁹⁰, M. Boonekamp¹⁴⁰, C.D. Booth⁹¹, A.G. Borbély⁵⁵, H.M. Borecka-Bielska¹⁰⁷, L.S. Borgna⁹², G. Borissov⁸⁷, D. Bortoletto¹³⁰, D. Boscherini^{21b}, M. Bosman¹², J.D. Bossio Sola³⁴, K. Bouaouda^{33a}, J. Boudreau¹³⁴, E.V. Bouhova-Thacker⁸⁷, D. Boumediene³⁶, R. Bouquet¹³¹, A. Boveia¹²³, J. Boyd³⁴, D. Boye²⁷, I.R. Boyko⁷⁷, A.J. Bozson⁹¹, J. Bracinik¹⁹, N. Brahimi^{58d,58c}, G. Brandt¹⁷⁷, O. Brandt³⁰, F. Braren⁴⁴, B. Brau¹⁰⁰, J.E. Brau¹²⁷, W.D. Breaden Madden⁵⁵, K. Brendlinger⁴⁴, R. Brenner¹⁷⁵, L. Brenner³⁴, R. Brenner¹⁶⁷, S. Bressler¹⁷⁵, B. Brickwedde⁹⁷, D.L. Briglin¹⁹, D. Britton⁵⁵, D. Britzger¹¹², I. Brock²², R. Brock¹⁰⁴, G. Brooijmans³⁷, W.K. Brooks^{142d}, E. Brost²⁷, P.A. Bruckman de Renstrom⁸², B. Brüers⁴⁴, D. Bruncko^{26b}, A. Bruni^{21b}, G. Bruni^{21b}, M. Bruschi^{21b}, N. Bruscino^{70a,70b}, L. Bryngemark¹⁴⁹, T. Buanes¹⁵, Q. Buat¹⁵¹, P. Buchholz¹⁴⁷, A.G. Buckley⁵⁵, I.A. Budagov⁷⁷, M.K. Bugge¹²⁹, O. Bulekov¹⁰⁹, B.A. Bullard⁵⁷, T.J. Burch¹¹⁷, S. Burdin⁸⁸, C.D. Burgard⁴⁴, A.M. Burger¹²⁵, B. Burghgrave⁷, J.T.P. Burr⁴⁴, C.D. Burton¹⁰, J.C. Burzynski¹⁰⁰, V. Büscher⁹⁷, P.J. Bussey⁵⁵, J.M. Butler²³, C.M. Buttar⁵⁵, J.M. Butterworth⁹², W. Buttinger¹³⁹, C.J. Buxo Vazquez¹⁰⁴, A.R. Buzykaev^{118b,118a}, G. Cabras^{21b}, S. Cabrera Urbán¹⁶⁹, D. Caforio⁵⁴, H. Cai¹³⁴, V.M.M. Cairo¹⁴⁹, O. Cakir^{3a}, N. Calace³⁴, P. Calafiura¹⁶, G. Calderini¹³¹, P. Calfayan⁶³, G. Callea⁵⁵, L.P. Caloba^{78b}, S. Calvente Lopez⁹⁶, D. Calvet³⁶, S. Calvet³⁶, T.P. Calvet⁹⁹, M. Calvetti^{69a,69b}, R. Camacho Toro¹³¹, S. Camarda³⁴, D. Camarero Munoz⁹⁶, P. Camarri^{71a,71b}, M.T. Camerlingo^{72a,72b}, D. Cameron¹²⁹, C. Camincher¹⁷¹, M. Campanelli⁹², A. Camplani³⁸, V. Canale^{67a,67b}, A. Canesse¹⁰¹, M. Cano Bret⁷⁵, J. Cantero¹²⁵, Y. Cao¹⁶⁸, F. Capocasa²⁴, M. Capua^{39b,39a}, A. Carbone^{66a,66b}, R. Cardarelli^{71a}, F. Cardillo¹⁶⁹, G. Carducci^{39b,39a}, T. Carli³⁴, G. Carlino^{67a}, B.T. Carlson¹³⁴, E.M. Carlson^{171,163a}, L. Carminati^{66a,66b}, M. Carnesale^{70a,70b}, R.M.D. Carney¹⁴⁹, S. Caron¹¹⁵, E. Carquin^{142d}, S. Carrá⁴⁴, G. Carratta^{21b,21a}, J.W.S. Carter¹⁶², T.M. Carter⁴⁸, D. Casadei^{31c}, M.P. Casado^{12,h}, A.F. Casha¹⁶², E.G. Castiglia¹⁷⁸, F.L. Castillo^{59a}, L. Castillo Garcia¹², V. Castillo Gimenez¹⁶⁹, N.F. Castro^{135a,135e}, A. Catinaccio³⁴, J.R. Catmore¹²⁹, A. Cattai³⁴, V. Cavaliere²⁷, N. Cavalli^{21b,21a}, V. Cavasinni^{69a,69b}, E. Celebi^{11b}, F. Celli¹³⁰, M.S. Centonze^{65a,65b}, K. Cerny¹²⁶, A.S. Cerqueira^{78a}, A. Cerri¹⁵²,

L. Cerrito ^{71a,71b}, F. Cerutti ¹⁶, A. Cervelli ^{21b}, S.A. Cetin ^{11b}, Z. Chadi ^{33a}, D. Chakraborty ¹¹⁷, M. Chala ^{135f}, J. Chan ¹⁷⁶, W.S. Chan ¹¹⁶, W.Y. Chan ⁸⁸, J.D. Chapman ³⁰, B. Chargeishvili ^{155b}, D.G. Charlton ¹⁹, T.P. Charman ⁹⁰, M. Chatterjee ¹⁸, S. Chekanov ⁵, S.V. Chekulaev ^{163a}, G.A. Chelkov ^{77,ag}, A. Chen ¹⁰³, B. Chen ¹⁵⁷, C. Chen ^{58a}, C.H. Chen ⁷⁶, H. Chen ^{13c}, H. Chen ²⁷, J. Chen ^{58c}, J. Chen ³⁷, J. Chen ²⁴, S. Chen ¹³², S.J. Chen ^{13c}, X. Chen ^{58c}, X. Chen ^{13b}, Y. Chen ^{58a}, Y.-H. Chen ⁴⁴, C.L. Cheng ¹⁷⁶, H.C. Cheng ^{60a}, H.J. Cheng ^{13a}, A. Cheplakov ⁷⁷, E. Cheremushkina ⁴⁴, E. Cherepanova ⁷⁷, R. Cherkaoui El Moursli ^{33e}, E. Cheu ⁶, K. Cheung ⁶¹, L. Chevalier ¹⁴⁰, V. Chiarella ⁴⁹, G. Chiarelli ^{69a}, G. Chiodini ^{65a}, A.S. Chisholm ¹⁹, A. Chitan ^{25b}, Y.H. Chiu ¹⁷¹, M.V. Chizhov ^{77,t}, K. Choi ¹⁰, A.R. Chomont ^{70a,70b}, Y. Chou ¹⁰⁰, Y.S. Chow ¹¹⁶, L.D. Christopher ^{31f}, M.C. Chu ^{60a}, X. Chu ^{13a,13d}, J. Chudoba ¹³⁶, J.J. Chwastowski ⁸², D. Cieri ¹¹², K.M. Ciesla ⁸², V. Cindro ⁸⁹, I.A. Cioară ^{25b}, A. Ciocio ¹⁶, F. Ciroto ^{67a,67b}, Z.H. Citron ^{175,l}, M. Citterio ^{66a}, D.A. Ciubotaru ^{25b}, B.M. Ciungu ¹⁶², A. Clark ⁵², P.J. Clark ⁴⁸, J.M. Clavijo Columbie ⁴⁴, S.E. Clawson ⁹⁸, C. Clement ^{43a,43b}, L. Clissa ^{21b,21a}, Y. Coadou ⁹⁹, M. Cobal ^{64a,64c}, A. Coccaro ^{53b}, J. Cochran ⁷⁶, R.F. Coelho Barrue ^{135a}, R. Coelho Lopes De Sa ¹⁰⁰, S. Coelli ^{66a}, H. Cohen ¹⁵⁷, A.E.C. Coimbra ³⁴, B. Cole ³⁷, J. Collot ⁵⁶, P. Conde Muiño ^{135a,135h}, S.H. Connell ^{31c}, I.A. Connolly ⁵⁵, E.I. Conroy ¹³⁰, F. Conventi ^{67a,am}, H.G. Cooke ¹⁹, A.M. Cooper-Sarkar ¹³⁰, F. Cormier ¹⁷⁰, L.D. Corpe ³⁴, M. Corradi ^{70a,70b}, E.E. Corrigan ⁹⁴, F. Corriveau ^{101,aa}, M.J. Costa ¹⁶⁹, F. Costanza ⁴, D. Costanzo ¹⁴⁵, B.M. Cote ¹²³, G. Cowan ⁹¹, J.W. Cowley ³⁰, K. Cranmer ¹²¹, S. Crépe-Renaudin ⁵⁶, F. Crescioli ¹³¹, M. Cristinziani ¹⁴⁷, M. Cristoforetti ^{73a,73b,b}, V. Croft ¹⁶⁵, G. Crosetti ^{39b,39a}, A. Cueto ³⁴, T. Cuhadar Donszelmann ¹⁶⁶, H. Cui ^{13a,13d}, A.R. Cukierman ¹⁴⁹, W.R. Cunningham ⁵⁵, P. Czodrowski ³⁴, M.M. Czurylo ^{59b}, M.J. Da Cunha Sargedas De Sousa ^{58a}, J.V. Da Fonseca Pinto ^{78b}, C. Da Via ⁹⁸, W. Dabrowski ^{81a}, T. Dado ⁴⁵, S. Dahbi ^{31f}, T. Dai ¹⁰³, C. Dallapiccola ¹⁰⁰, M. Dam ³⁸, G. D'amen ²⁷, V. D'Amico ^{72a,72b}, J. Damp ⁹⁷, J.R. Dandoy ¹³², M.F. Daneri ²⁸, M. Danninger ¹⁴⁸, V. Dao ³⁴, G. Darbo ^{53b}, S. Darmora ⁵, A. Dattagupta ¹²⁷, S. D'Auria ^{66a,66b}, C. David ^{163b}, T. Davidek ¹³⁸, D.R. Davis ⁴⁷, B. Davis-Purcell ³², I. Dawson ⁹⁰, K. De ⁷, R. De Asmundis ^{67a}, M. De Beurs ¹¹⁶, S. De Castro ^{21b,21a}, N. De Groot ¹¹⁵, P. de Jong ¹¹⁶, H. De la Torre ¹⁰⁴, A. De Maria ^{13c}, D. De Pedis ^{70a}, A. De Salvo ^{70a}, U. De Sanctis ^{71a,71b}, M. De Santis ^{71a,71b}, A. De Santo ¹⁵², J.B. De Vivie De Regie ⁵⁶, D.V. Dedovich ⁷⁷, J. Degen ¹¹⁶, A.M. Deiana ⁴⁰, J. Del Peso ⁹⁶, Y. Delabat Diaz ⁴⁴, F. Deliot ¹⁴⁰, C.M. Delitzsch ⁶, M. Della Pietra ^{67a,67b}, D. Della Volpe ⁵², A. Dell'Acqua ³⁴, L. Dell'Asta ^{66a,66b}, M. Delmastro ⁴, P.A. Delsart ⁵⁶, S. Demers ¹⁷⁸, M. Demichev ⁷⁷, S.P. Denisov ¹¹⁹, L. D'Eramo ¹¹⁷, D. Derendarz ⁸², J.E. Derkaoui ^{33d}, F. Derue ¹³¹, P. Dervan ⁸⁸, K. Desch ²², K. Dette ¹⁶², C. Deutsch ²², P.O. Deviveiros ³⁴, F.A. Di Bello ^{70a,70b}, A. Di Ciaccio ^{71a,71b}, L. Di Ciaccio ⁴, C. Di Donato ^{67a,67b}, A. Di Girolamo ³⁴, G. Di Gregorio ^{69a,69b}, A. Di Luca ^{73a,73b}, B. Di Micco ^{72a,72b}, R. Di Nardo ^{72a,72b}, C. Diaconu ⁹⁹, F.A. Dias ¹¹⁶, T. Dias Do Vale ^{135a}, M.A. Diaz ^{142a}, F.G. Diaz Capriles ²², J. Dickinson ¹⁶, M. Didenko ¹⁶⁹, E.B. Diehl ¹⁰³, J. Dietrich ¹⁷, S. Díez Cornell ⁴⁴, C. Diez Pardos ¹⁴⁷, A. Dimitrievska ¹⁶, W. Ding ^{13b}, J. Dingfelder ²², I.-M. Dinu ^{25b}, S.J. Dittmeier ^{59b}, F. Dittus ³⁴, F. Djama ⁹⁹, T. Djobava ^{155b}, J.I. Djuvsland ¹⁵, M.A.B. Do Vale ¹⁴³, D. Dodsworth ²⁴, C. Doglioni ⁹⁴, J. Dolejsi ¹³⁸, Z. Dolezal ¹³⁸, M. Donadelli ^{78c}, B. Dong ^{58c}, J. Donini ³⁶, A. D'Onofrio ^{13c}, M. D'Onofrio ⁸⁸, J. Dopke ¹³⁹, A. Doria ^{67a}, M.T. Dova ⁸⁶, A.T. Doyle ⁵⁵, E. Drechsler ¹⁴⁸, E. Dreyer ¹⁴⁸, T. Dreyer ⁵¹, A.S. Drobac ¹⁶⁵, D. Du ^{58b}, T.A. du Pree ¹¹⁶, F. Dubinin ¹⁰⁸, M. Dubovsky ^{26a}, A. Dubreuil ⁵², E. Duchovni ¹⁷⁵, G. Duckeck ¹¹¹, O.A. Ducu ^{34,25b}, D. Duda ¹¹², A. Dudarev ³⁴, M. D'uffizi ⁹⁸, L. Duflot ⁶², M. Dührssen ³⁴, C. Dülzen ¹⁷⁷, A.E. Dumitriu ^{25b}, M. Dunford ^{59a}, S. Dungs ⁴⁵, K. Dunne ^{43a,43b}, A. Duperrin ⁹⁹, H. Duran Yildiz ^{3a}, M. Düren ⁵⁴, A. Durglishvili ^{155b}, B. Dutta ⁴⁴, B.L. Dwyer ¹¹⁷, G.I. Dyckes ¹³², M. Dyndal ^{81a}, S. Dysch ⁹⁸, B.S. Dzierdzic ⁸², B. Eckerova ^{26a}, M.G. Eggleston ⁴⁷, E. Egidio Purcino De Souza ^{78b}, L.F. Ehrke ⁵², T. Eifert ⁷, G. Eigen ¹⁵, K. Einsweiler ¹⁶, T. Ekelof ¹⁶⁷, Y. El Ghazali ^{33b}, H. El Jarrari ^{33e}, A. El Moussaouy ^{33a}, V. Ellajosyula ¹⁶⁷, M. Ellert ¹⁶⁷, F. Ellinghaus ¹⁷⁷, A.A. Elliot ⁹⁰, N. Ellis ³⁴, J. Elmsheuser ²⁷, M. Elsing ³⁴, D. Emelianov ¹³⁹, A. Emerman ³⁷, Y. Enari ¹⁵⁹, J. Erdmann ⁴⁵, A. Ereditato ¹⁸, P.A. Erland ⁸², M. Errenst ¹⁷⁷, M. Escalier ⁶², C. Escobar ¹⁶⁹, O. Estrada Pastor ¹⁶⁹, E. Etzion ¹⁵⁷, G. Evans ^{135a}, H. Evans ⁶³, M.O. Evans ¹⁵², A. Ezhilov ¹³³, F. Fabbri ⁵⁵, L. Fabbri ^{21b,21a}, V. Fabiani ¹¹⁵, G. Facini ¹⁷³, V. Fadeyev ¹⁴¹, R.M. Fakhruddinov ¹¹⁹, S. Falciano ^{70a}, P.J. Falke ²², S. Falke ³⁴, J. Faltova ¹³⁸, Y. Fan ^{13a}, Y. Fang ^{13a}, Y. Fang ^{13a}, G. Fanourakis ⁴², M. Fanti ^{66a,66b}, M. Faraj ^{58c}, A. Farbin ⁷, A. Farilla ^{72a}, E.M. Farina ^{68a,68b}, T. Farooque ¹⁰⁴, S.M. Farrington ⁴⁸, P. Farthouat ³⁴, F. Fassi ^{33e}, D. Fassouliotis ⁸, M. Fauci Giannelli ^{71a,71b}, W.J. Fawcett ³⁰, L. Fayard ⁶², O.L. Fedin ^{133,q}, M. Feickert ¹⁶⁸, L. Feligioni ⁹⁹, A. Fell ¹⁴⁵, C. Feng ^{58b}, M. Feng ^{13b}, M.J. Fenton ¹⁶⁶, A.B. Fenyuk ¹¹⁹, S.W. Ferguson ⁴¹, J. Ferrando ⁴⁴, A. Ferrari ¹⁶⁷, P. Ferrari ¹¹⁶, R. Ferrari ^{68a}, D. Ferrere ⁵², C. Ferretti ¹⁰³, F. Fiedler ⁹⁷, A. Filipčić ⁸⁹, F. Filthaut ¹¹⁵,

M.C.N. Fiolhais ^{135a,135c,a}, L. Fiorini ¹⁶⁹, F. Fischer ¹⁴⁷, W.C. Fisher ¹⁰⁴, T. Fitschen ¹⁹, I. Fleck ¹⁴⁷,
 P. Fleischmann ¹⁰³, T. Flick ¹⁷⁷, B.M. Flierl ¹¹¹, L. Flores ¹³², L.R. Flores Castillo ^{60a}, F.M. Follega ^{73a,73b},
 N. Fomin ¹⁵, J.H. Foo ¹⁶², G.T. Forcolin ^{73a,73b}, B.C. Forland ⁶³, A. Formica ¹⁴⁰, F.A. Förster ¹², A.C. Forti ⁹⁸,
 E. Fortin ⁹⁹, M.G. Foti ¹³⁰, D. Fournier ⁶², H. Fox ⁸⁷, P. Francavilla ^{69a,69b}, S. Francescato ^{70a,70b},
 M. Franchini ^{21b,21a}, S. Franchino ^{59a}, D. Francis ³⁴, L. Franco ⁴, L. Franconi ¹⁸, M. Franklin ⁵⁷,
 G. Frattari ^{70a,70b}, A.C. Freegard ⁹⁰, P.M. Freeman ¹⁹, B. Freund ¹⁰⁷, W.S. Freund ^{78b}, E.M. Freundlich ⁴⁵,
 D. Froidevaux ³⁴, J.A. Frost ¹³⁰, Y. Fu ^{58a}, M. Fujimoto ¹²², E. Fullana Torregrosa ¹⁶⁹, J. Fuster ¹⁶⁹,
 A. Gabrielli ^{21b,21a}, A. Gabrielli ³⁴, P. Gadow ⁴⁴, G. Gagliardi ^{53b,53a}, L.G. Gagnon ¹⁶, G.E. Gallardo ¹³⁰,
 E.J. Gallas ¹³⁰, B.J. Gallop ¹³⁹, R. Gamboa Goni ⁹⁰, K.K. Gan ¹²³, S. Ganguly ¹⁷⁵, J. Gao ^{58a}, Y. Gao ⁴⁸,
 Y.S. Gao ^{29,n}, F.M. Garay Walls ^{142a}, C. García ¹⁶⁹, J.E. García Navarro ¹⁶⁹, J.A. García Pascual ^{13a},
 M. Garcia-Sciveres ¹⁶, R.W. Gardner ³⁵, D. Garg ⁷⁵, S. Gargiulo ⁵⁰, C.A. Garner ¹⁶², V. Garonne ¹²⁹,
 S.J. Gasirowski ¹⁴⁴, P. Gaspar ^{78b}, G. Gaudio ^{68a}, P. Gauzzi ^{70a,70b}, I.L. Gavrilenko ¹⁰⁸, A. Gavrilyuk ¹²⁰,
 C. Gay ¹⁷⁰, G. Gaycken ⁴⁴, E.N. Gazis ⁹, A.A. Geanta ^{25b}, C.M. Gee ¹⁴¹, C.N.P. Gee ¹³⁹, J. Geisen ⁹⁴,
 M. Geisen ⁹⁷, C. Gemme ^{53b}, M.H. Genest ⁵⁶, S. Gentile ^{70a,70b}, S. George ⁹¹, W.F. George ¹⁹, T. Gerialis ⁴²,
 L.O. Gerlach ⁵¹, P. Gessinger-Befurt ³⁴, M. Ghasemi Bostanabad ¹⁷¹, M. Ghneimat ¹⁴⁷, A. Ghosh ¹⁶⁶,
 A. Ghosh ⁷⁵, B. Giacobbe ^{21b}, S. Giagu ^{70a,70b}, N. Giangiacomi ¹⁶², P. Giannetti ^{69a}, A. Giannini ^{67a,67b},
 S.M. Gibson ⁹¹, M. Gignac ¹⁴¹, D.T. Gil ^{81b}, B.J. Gilbert ³⁷, D. Gillberg ³², G. Gilles ¹¹⁶, N.E.K. Gillwald ⁴⁴,
 D.M. Gingrich ^{2,al}, M.P. Giordani ^{64a,64c}, P.F. Giraud ¹⁴⁰, G. Giugliarelli ^{64a,64c}, D. Giugni ^{66a}, F. Giuli ^{71a,71b},
 I. Gkialas ^{8,i}, P. Gkountoumis ⁹, L.K. Gladilin ¹¹⁰, C. Glasman ⁹⁶, G.R. Gledhill ¹²⁷, M. Glisic ¹²⁷,
 I. Gnesi ^{39b,d}, M. Goblirsch-Kolb ²⁴, D. Godin ¹⁰⁷, S. Goldfarb ¹⁰², T. Golling ⁵², D. Golubkov ¹¹⁹,
 J.P. Gombas ¹⁰⁴, A. Gomes ^{135a,135b}, R. Goncalves Gama ⁵¹, R. Gonçalves ^{135a,135c}, G. Gonella ¹²⁷,
 L. Gonella ¹⁹, A. Gongadze ⁷⁷, F. Gonnella ¹⁹, J.L. Gonski ³⁷, S. González de la Hoz ¹⁶⁹,
 S. Gonzalez Fernandez ¹², R. Gonzalez Lopez ⁸⁸, C. Gonzalez Renteria ¹⁶, R. Gonzalez Suarez ¹⁶⁷,
 S. Gonzalez-Sevilla ⁵², G.R. Gonzalvo Rodriguez ¹⁶⁹, R.Y. González Andana ^{142a}, L. Goossens ³⁴,
 N.A. Gorasia ¹⁹, P.A. Gorbounov ¹²⁰, H.A. Gordon ²⁷, B. Gorini ³⁴, E. Gorini ^{65a,65b}, A. Gorišek ⁸⁹,
 A.T. Goshaw ⁴⁷, M.I. Gostkin ⁷⁷, C.A. Gottardo ¹¹⁵, M. Gouighri ^{33b}, V. Goumarre ⁴⁴, A.G. Goussiou ¹⁴⁴,
 N. Govender ^{31c}, C. Goy ⁴, I. Grabowska-Bold ^{81a}, K. Graham ³², E. Gramstad ¹²⁹, S. Grancagnolo ¹⁷,
 M. Grandi ¹⁵², V. Gratchev ¹³³, P.M. Gravila ^{25f}, F.G. Gravili ^{65a,65b}, H.M. Gray ¹⁶, C. Grefe ²², I.M. Gregor ⁴⁴,
 P. Grenier ¹⁴⁹, K. Grevtsov ⁴⁴, C. Grieco ¹², N.A. Grieser ¹²⁴, A.A. Grillo ¹⁴¹, K. Grimm ^{29,m}, S. Grinstein ^{12,x},
 J.-F. Grivaz ⁶², S. Groh ⁹⁷, E. Gross ¹⁷⁵, J. Grosse-Knetter ⁵¹, Z.J. Grout ⁹², C. Grud ¹⁰³, A. Grummer ¹¹⁴,
 J.C. Grundy ¹³⁰, L. Guan ¹⁰³, W. Guan ¹⁷⁶, C. Gubbels ¹⁷⁰, J. Guenther ³⁴, J.G.R. Guerrero Rojas ¹⁶⁹,
 F. Guescini ¹¹², D. Guest ¹⁷, R. Gugel ⁹⁷, A. Guida ⁴⁴, T. Guillemin ⁴, S. Guindon ³⁴, J. Guo ^{58c}, L. Guo ⁶²,
 Y. Guo ¹⁰³, R. Gupta ⁴⁴, S. Gurbuz ²², G. Gustavino ¹²⁴, M. Guth ⁵², P. Gutierrez ¹²⁴,
 L.F. Gutierrez Zagazeta ¹³², C. Gutschow ⁹², C. Guyot ¹⁴⁰, C. Gwenlan ¹³⁰, C.B. Gwilliam ⁸⁸, E.S. Haaland ¹²⁹,
 A. Haas ¹²¹, M. Habedank ¹⁷, C. Haber ¹⁶, H.K. Hadavand ⁷, A. Hadeef ⁹⁷, M. Haleem ¹⁷², J. Haley ¹²⁵,
 J.J. Hall ¹⁴⁵, G. Halladjian ¹⁰⁴, G.D. Hallewell ⁹⁹, L. Halser ¹⁸, K. Hamano ¹⁷¹, H. Hamdaoui ^{33e}, M. Hamer ²²,
 G.N. Hamity ⁴⁸, K. Han ^{58a}, L. Han ^{13c}, L. Han ^{58a}, S. Han ¹⁶, Y.F. Han ¹⁶², K. Hanagaki ^{79,v}, M. Hance ¹⁴¹,
 M.D. Hank ³⁵, R. Hankache ⁹⁸, E. Hansen ⁹⁴, J.B. Hansen ³⁸, J.D. Hansen ³⁸, M.C. Hansen ²², P.H. Hansen ³⁸,
 K. Hara ¹⁶⁴, T. Harenberg ¹⁷⁷, S. Harkusha ¹⁰⁵, Y.T. Harris ¹³⁰, P.F. Harrison ¹⁷³, N.M. Hartman ¹⁴⁹,
 N.M. Hartmann ¹¹¹, Y. Hasegawa ¹⁴⁶, A. Hasib ⁴⁸, S. Hassani ¹⁴⁰, S. Haug ¹⁸, R. Hauser ¹⁰⁴, M. Havranek ¹³⁷,
 C.M. Hawkes ¹⁹, R.J. Hawkins ³⁴, S. Hayashida ¹¹³, D. Hayden ¹⁰⁴, C. Hayes ¹⁰³, R.L. Hayes ¹⁷⁰,
 C.P. Hays ¹³⁰, J.M. Hays ⁹⁰, H.S. Hayward ⁸⁸, S.J. Haywood ¹³⁹, F. He ^{58a}, Y. He ¹⁶⁰, Y. He ¹³¹, M.P. Heath ⁴⁸,
 V. Hedberg ⁹⁴, A.L. Heggelund ¹²⁹, N.D. Hehir ⁹⁰, C. Heidegger ⁵⁰, K.K. Heidegger ⁵⁰, W.D. Heidorn ⁷⁶,
 J. Heilman ³², S. Heim ⁴⁴, T. Heim ¹⁶, B. Heinemann ^{44,aj}, J.G. Heinlein ¹³², J.J. Heinrich ¹²⁷, L. Heinrich ³⁴,
 J. Hejbal ¹³⁶, L. Helary ⁴⁴, A. Held ¹²¹, S. Hellesund ¹²⁹, C.M. Helling ¹⁴¹, S. Hellman ^{43a,43b}, C. Helsens ³⁴,
 R.C.W. Henderson ⁸⁷, L. Henkelmann ³⁰, A.M. Henriques Correia ³⁴, H. Herde ¹⁴⁹,
 Y. Hernández Jiménez ¹⁵¹, H. Herr ⁹⁷, M.G. Herrmann ¹¹¹, T. Herrmann ⁴⁶, G. Herten ⁵⁰,
 R. Hertenberger ¹¹¹, L. Hervas ³⁴, N.P. Hessey ^{163a}, H. Hibi ⁸⁰, S. Higashino ⁷⁹, E. Higón-Rodríguez ¹⁶⁹,
 K.K. Hill ²⁷, K.H. Hiller ⁴⁴, S.J. Hillier ¹⁹, M. Hils ⁴⁶, I. Hinchliffe ¹⁶, F. Hinterkeuser ²², M. Hirose ¹²⁸,
 S. Hirose ¹⁶⁴, D. Hirschbuehl ¹⁷⁷, B. Hiti ⁸⁹, O. Hladik ¹³⁶, J. Hobbs ¹⁵¹, R. Hobincu ^{25e}, N. Hod ¹⁷⁵,
 M.C. Hodgkinson ¹⁴⁵, B.H. Hodgkinson ³⁰, A. Hoecker ³⁴, J. Hofer ⁴⁴, D. Hohn ⁵⁰, T. Holm ²², T.R. Holmes ³⁵,
 M. Holzbock ¹¹², L.B.A.H. Hommels ³⁰, B.P. Honan ⁹⁸, J. Hong ^{58c}, T.M. Hong ¹³⁴, J.C. Honig ⁵⁰, A. Hönle ¹¹²,
 B.H. Hooberman ¹⁶⁸, W.H. Hopkins ⁵, Y. Horii ¹¹³, P. Horn ⁴⁶, L.A. Horyn ³⁵, S. Hou ¹⁵⁴, J. Howarth ⁵⁵,

J. Hoya⁸⁶, M. Hrabovsky¹²⁶, A. Hrynevich¹⁰⁶, T. Hryn'ova⁴, P.J. Hsu⁶¹, S.-C. Hsu¹⁴⁴, Q. Hu³⁷, S. Hu^{58c}, Y.F. Hu^{13a,13d,an}, D.P. Huang⁹², X. Huang^{13c}, Y. Huang^{58a}, Y. Huang^{13a}, Z. Hubacek¹³⁷, F. Hubaut⁹⁹, M. Huebner²², F. Huegging²², T.B. Huffman¹³⁰, M. Huhtinen³⁴, R. Hulsken⁵⁶, N. Huseynov^{77,ab}, J. Huston¹⁰⁴, J. Huth⁵⁷, R. Hyneman¹⁴⁹, S. Hyrych^{26a}, G. Iacobucci⁵², G. Iakovidis²⁷, I. Ibragimov¹⁴⁷, L. Iconomidou-Fayard⁶², P. Iengo³⁴, R. Iguchi¹⁵⁹, T. Iizawa⁵², Y. Ikegami⁷⁹, A. Ilg¹⁸, N. Ilic¹⁶², H. Imam^{33a}, T. Ingebretsen Carlson^{43a,43b}, G. Introzzi^{68a,68b}, M. Iodice^{72a}, V. Ippolito^{70a,70b}, M. Ishino¹⁵⁹, W. Islam¹²⁵, C. Issever^{17,44}, S. Istin^{11c,ao}, J.M. Iturbe Ponce^{60a}, R. Iuppa^{73a,73b}, A. Ivina¹⁷⁵, J.M. Izen⁴¹, V. Izzo^{67a}, P. Jacka¹³⁶, P. Jackson¹, R.M. Jacobs⁴⁴, B.P. Jaeger¹⁴⁸, C.S. Jagfeld¹¹¹, G. Jäkel¹⁷⁷, K. Jakobs⁵⁰, T. Jakoubek¹⁷⁵, J. Jamieson⁵⁵, K.W. Janas^{81a}, G. Jarlskog⁹⁴, A.E. Jaspan⁸⁸, N. Javadov^{77,ab}, T. Javůrek³⁴, M. Javurkova¹⁰⁰, F. Jeanneau¹⁴⁰, L. Jeanty¹²⁷, J. Jejelava^{155a,ac}, P. Jenni^{50,e}, S. Jézéquel⁴, J. Jia¹⁵¹, Z. Jia^{13c}, Y. Jiang^{58a}, S. Jiggins⁵⁰, J. Jimenez Pena¹¹², S. Jin^{13c}, A. Jinaru^{25b}, O. Jinnouchi¹⁶⁰, H. Jivan^{31f}, P. Johansson¹⁴⁵, K.A. Johns⁶, C.A. Johnson⁶³, D.M. Jones³⁰, E. Jones¹⁷³, R.W.L. Jones⁸⁷, T.J. Jones⁸⁸, J. Jovicevic⁵¹, X. Ju¹⁶, J.J. Junggeburth³⁴, A. Juste Rozas^{12,x}, S. Kabana^{142c}, A. Kaczmarska⁸², M. Kado^{70a,70b}, H. Kagan¹²³, M. Kagan¹⁴⁹, A. Kahn³⁷, C. Kahra⁹⁷, T. Kaji¹⁷⁴, E. Kajomovitz¹⁵⁶, C.W. Kalderon²⁷, A. Kamenshchikov¹¹⁹, M. Kaneda¹⁵⁹, N.J. Kang¹⁴¹, S. Kang⁷⁶, Y. Kano¹¹³, J. Kanzaki⁷⁹, D. Kar^{31f}, K. Karava¹³⁰, M.J. Kareem^{163b}, I. Karkanas¹⁵⁸, S.N. Karpov⁷⁷, Z.M. Karpova⁷⁷, V. Kartvelishvili⁸⁷, A.N. Karyukhin¹¹⁹, E. Kasimi¹⁵⁸, C. Kato^{58d}, J. Katzy⁴⁴, K. Kawade¹⁴⁶, K. Kawagoe⁸⁵, T. Kawaguchi¹¹³, T. Kawamoto¹⁴⁰, G. Kawamura⁵¹, E.F. Kay¹⁷¹, F.I. Kaya¹⁶⁵, S. Kazakos¹², V.F. Kazanin^{118b,118a}, Y. Ke¹⁵¹, J.M. Keaveney^{31a}, R. Keeler¹⁷¹, J.S. Keller³², D. Kelsey¹⁵², J.J. Kempster¹⁹, J. Kendrick¹⁹, K.E. Kennedy³⁷, O. Kepka¹³⁶, S. Kersten¹⁷⁷, B.P. Kerševan⁸⁹, S. Ketabchi Haghighat¹⁶², M. Khandoga¹³¹, A. Khanov¹²⁵, A.G. Kharlamov^{118b,118a}, T. Kharlamova^{118b,118a}, E.E. Khoda¹⁴⁴, T.J. Khoo¹⁷, G. Khoriauli¹⁷², E. Khramov⁷⁷, J. Khubua^{155b}, S. Kido⁸⁰, M. Kiehn³⁴, A. Kilgallon¹²⁷, E. Kim¹⁶⁰, Y.K. Kim³⁵, N. Kimura⁹², A. Kirchhoff⁵¹, D. Kirchmeier⁴⁶, C. Kirfel²², J. Kirk¹³⁹, A.E. Kiryunin¹¹², T. Kishimoto¹⁵⁹, D.P. Kisliuk¹⁶², V. Kitali⁴⁴, C. Kitsaki⁹, O. Kivernyk²², T. Klapdor-Kleingrothaus⁵⁰, M. Klassen^{59a}, C. Klein³², L. Klein¹⁷², M.H. Klein¹⁰³, M. Klein⁸⁸, U. Klein⁸⁸, P. Klimek³⁴, A. Klimentov²⁷, F. Klimpel³⁴, T. Klingl²², T. Klioutchnikova³⁴, F.F. Klitzner¹¹¹, P. Kluit¹¹⁶, S. Kluth¹¹², E. Kneringer⁷⁴, T.M. Knight¹⁶², A. Knue⁵⁰, D. Kobayashi⁸⁵, M. Kobel⁴⁶, M. Kocian¹⁴⁹, T. Kodama¹⁵⁹, P. Kodys¹³⁸, D.M. Koeck¹⁵², P.T. Koenig²², T. Koffas³², N.M. Köhler³⁴, M. Kolb¹⁴⁰, I. Koletsou⁴, T. Komarek¹²⁶, K. Köneke⁵⁰, A.X.Y. Kong¹, T. Kono¹²², V. Konstantinides⁹², N. Konstantinidis⁹², B. Konya⁹⁴, R. Kopeliansky⁶³, S. Koperny^{81a}, K. Korcyl⁸², K. Kordas¹⁵⁸, G. Koren¹⁵⁷, A. Korn⁹², S. Korn⁵¹, I. Korolkov¹², E.V. Korolkova¹⁴⁵, N. Korotkova¹¹⁰, B. Kortman¹¹⁶, O. Kortner¹¹², S. Kortner¹¹², W.H. Kostecka¹¹⁷, V.V. Kostyukhin^{145,161}, A. Kotschechagia⁶², A. Kotwal⁴⁷, A. Koulouris³⁴, A. Kourkoumeli-Charalampidi^{68a,68b}, C. Kourkoumelis⁸, E. Kourlitis⁵, O. Kovanda¹⁵², R. Kowalewski¹⁷¹, W. Kozanecki¹⁴⁰, A.S. Kozhin¹¹⁹, V.A. Kramarenko¹¹⁰, G. Kramberger⁸⁹, D. Krasnopevtsev^{58a}, M.W. Krasny¹³¹, A. Krasznahorkay³⁴, J.A. Kremer⁹⁷, J. Kretzschmar⁸⁸, K. Kreul¹⁷, P. Krieger¹⁶², F. Krieter¹¹¹, S. Krishnamurthy¹⁰⁰, A. Krishnan^{59b}, M. Krivos¹³⁸, K. Krizka¹⁶, K. Kroeninger⁴⁵, H. Kroha¹¹², J. Kroll¹³⁶, J. Kroll¹³², K.S. Krowpman¹⁰⁴, U. Kruchonak⁷⁷, H. Krüger²², N. Krumnack⁷⁶, M.C. Kruse⁴⁷, J.A. Krzysiak⁸², A. Kubota¹⁶⁰, O. Kuchinskaia¹⁶¹, S. Kuday^{3b}, D. Kuechler⁴⁴, J.T. Kuechler⁴⁴, S. Kuehn³⁴, T. Kuhl⁴⁴, V. Kukhtin⁷⁷, Y. Kulchitsky^{105,af}, S. Kuleshov^{142b}, M. Kumar^{31f}, N. Kumari⁹⁹, M. Kuna⁵⁶, A. Kupco¹³⁶, T. Kupfer⁴⁵, O. Kuprash⁵⁰, H. Kurashige⁸⁰, L.L. Kurchaninov^{163a}, Y.A. Kurochkin¹⁰⁵, A. Kurova¹⁰⁹, M.G. Kurth^{13a,13d}, E.S. Kuwertz³⁴, M. Kuze¹⁶⁰, A.K. Kvam¹⁴⁴, J. Kvita¹²⁶, T. Kwan¹⁰¹, K.W. Kwok^{60a}, C. Lacasta¹⁶⁹, F. Lacava^{70a,70b}, H. Lacker¹⁷, D. Lacour¹³¹, N.N. Lad⁹², E. Ladygin⁷⁷, R. Lafaye⁴, B. Laforge¹³¹, T. Lagouri^{142c}, S. Lai⁵¹, I.K. Lakomic^{81a}, N. Lalloue⁵⁶, J.E. Lambert¹²⁴, S. Lammers⁶³, W. Lampl⁶, C. Lampoudis¹⁵⁸, E. Lançon²⁷, U. Landgraf⁵⁰, M.P.J. Landon⁹⁰, V.S. Lang⁵⁰, J.C. Lange⁵¹, R.J. Langenberg¹⁰⁰, A.J. Lankford¹⁶⁶, F. Lanni²⁷, K. Lantzsch²², A. Lanza^{68a}, A. Lapertosa^{53b,53a}, J.F. Laporte¹⁴⁰, T. Lari^{66a}, F. Lasagni Manghi^{21b}, M. Lassnig³⁴, V. Latonova¹³⁶, T.S. Lau^{60a}, A. Laudrain⁹⁷, A. Laurier³², M. Lavorgna^{67a,67b}, S.D. Lawlor⁹¹, Z. Lawrence⁹⁸, M. Lazzaroni^{66a,66b}, B. Le⁹⁸, B. Leban⁸⁹, A. Lebedev⁷⁶, M. LeBlanc³⁴, T. LeCompte⁵, F. Ledroit-Guillon⁵⁶, A.C.A. Lee⁹², G.R. Lee¹⁵, L. Lee⁵⁷, S.C. Lee¹⁵⁴, S. Lee⁷⁶, L.L. Leeuw^{31c}, B. Lefebvre^{163a}, H.P. Lefebvre⁹¹, M. Lefebvre¹⁷¹, C. Leggett¹⁶, K. Lehmann¹⁴⁸, N. Lehmann¹⁸, G. Lehmann Miotto³⁴, W.A. Leight⁴⁴, A. Leisos^{158,w}, M.A.L. Leite^{78c}, C.E. Leitgeb⁴⁴, R. Leitner¹³⁸, K.J.C. Leney⁴⁰, T. Lenz²², S. Leone^{69a}, C. Leonidopoulos⁴⁸, A. Leopold¹³¹, C. Leroy¹⁰⁷, R. Les¹⁰⁴, C.G. Lester³⁰, M. Levchenko¹³³, J. Levêque⁴, D. Levin¹⁰³, L.J. Levinson¹⁷⁵, D.J. Lewis¹⁹, B. Li^{13b}, B. Li^{58b},

C. Li ^{58a}, C.-Q. Li ^{58c,58d}, H. Li ^{58a}, H. Li ^{58b}, J. Li ^{58c}, K. Li ¹⁴⁴, L. Li ^{58c}, M. Li ^{13a,13d}, Q.Y. Li ^{58a}, S. Li ^{58d,58c,c}, X. Li ⁴⁴, Y. Li ⁴⁴, Z. Li ^{58b}, Z. Li ¹³⁰, Z. Li ¹⁰¹, Z. Li ⁸⁸, Z. Liang ^{13a}, M. Liberatore ⁴⁴, B. Liberti ^{71a}, K. Lie ^{60c}, K. Lin ¹⁰⁴, R.A. Linck ⁶³, R.E. Lindley ⁶, J.H. Lindon ², A. Linss ⁴⁴, E. Lipeles ¹³², A. Lipniacka ¹⁵, T.M. Liss ^{168,ak}, A. Lister ¹⁷⁰, J.D. Little ⁷, B. Liu ^{13a}, B.X. Liu ¹⁴⁸, J.B. Liu ^{58a}, J.K.K. Liu ³⁵, K. Liu ^{58d,58c}, M. Liu ^{58a}, M.Y. Liu ^{58a}, P. Liu ^{13a}, X. Liu ^{58a}, Y. Liu ⁴⁴, Y. Liu ^{13c,13d}, Y.L. Liu ¹⁰³, Y.W. Liu ^{58a}, M. Livan ^{68a,68b}, A. Lleres ⁵⁶, J. Llorente Merino ¹⁴⁸, S.L. Lloyd ⁹⁰, E.M. Lobodzinska ⁴⁴, P. Loch ⁶, S. Loffredo ^{71a,71b}, T. Lohse ¹⁷, K. Lohwasser ¹⁴⁵, M. Lokajicek ¹³⁶, J.D. Long ¹⁶⁸, I. Longarini ^{70a,70b}, L. Longo ³⁴, R. Longo ¹⁶⁸, I. Lopez Paz ¹², A. Lopez Solis ⁴⁴, J. Lorenz ¹¹¹, N. Lorenzo Martinez ⁴, A.M. Lory ¹¹¹, A. Lösle ⁵⁰, X. Lou ^{43a,43b}, X. Lou ^{13a}, A. Lounis ⁶², J. Love ⁵, P.A. Love ⁸⁷, J.J. Lozano Bahilo ¹⁶⁹, G. Lu ^{13a}, M. Lu ^{58a}, S. Lu ¹³², Y.J. Lu ⁶¹, H.J. Lubatti ¹⁴⁴, C. Luci ^{70a,70b}, F.L. Lucio Alves ^{13c}, A. Lucotte ⁵⁶, F. Luehring ⁶³, I. Luise ¹⁵¹, L. Luminari ^{70a}, O. Lundberg ¹⁵⁰, B. Lund-Jensen ¹⁵⁰, N.A. Luongo ¹²⁷, M.S. Lutz ¹⁵⁷, D. Lynn ²⁷, H. Lyons ⁸⁸, R. Lysak ¹³⁶, E. Lytken ⁹⁴, F. Lyu ^{13a}, V. Lyubushkin ⁷⁷, T. Lyubushkina ⁷⁷, H. Ma ²⁷, L.L. Ma ^{58b}, Y. Ma ⁹², D.M. Mac Donell ¹⁷¹, G. Maccarrone ⁴⁹, C.M. Macdonald ¹⁴⁵, J.C. MacDonald ¹⁴⁵, R. Madar ³⁶, W.F. Mader ⁴⁶, M. Madugoda Ralalage Don ¹²⁵, N. Madysa ⁴⁶, J. Maeda ⁸⁰, T. Maeno ²⁷, M. Maerker ⁴⁶, V. Magerl ⁵⁰, J. Magro ^{64a,64c}, D.J. Mahon ³⁷, C. Maidantchik ^{78b}, A. Maio ^{135a,135b,135d}, K. Maj ^{81a}, O. Majersky ^{26a}, S. Majewski ¹²⁷, N. Makovec ⁶², B. Malaescu ¹³¹, Pa. Malecki ⁸², V.P. Maleev ¹³³, F. Malek ⁵⁶, D. Malito ^{39b,39a}, U. Mallik ⁷⁵, C. Malone ³⁰, S. Maltezos ⁹, S. Malyukov ⁷⁷, J. Mamuzic ¹⁶⁹, G. Mancini ⁴⁹, J.P. Mandalia ⁹⁰, I. Mandić ⁸⁹, L. Manhaes de Andrade Filho ^{78a}, I.M. Maniatis ¹⁵⁸, M. Manisha ¹⁴⁰, J. Manjarres Ramos ⁴⁶, K.H. Mankinen ⁹⁴, A. Mann ¹¹¹, A. Manousos ⁷⁴, B. Mansoulie ¹⁴⁰, I. Mantos ¹⁵⁸, S. Manzoni ¹¹⁶, A. Marantis ^{158,w}, L. Marchese ¹³⁰, G. Marchiori ¹³¹, M. Marcisovsky ¹³⁶, L. Marcocchia ^{71a,71b}, C. Marcon ⁹⁴, M. Marjanovic ¹²⁴, Z. Marshall ¹⁶, S. Marti-Garcia ¹⁶⁹, T.A. Martin ¹⁷³, V.J. Martin ⁴⁸, B. Martin dit Latour ¹⁵, L. Martinelli ^{70a,70b}, M. Martinez ^{12,x}, P. Martinez Agullo ¹⁶⁹, V.I. Martinez Outschoorn ¹⁰⁰, S. Martin-Haugh ¹³⁹, V.S. Martoiu ^{25b}, A.C. Martyniuk ⁹², A. Marzin ³⁴, S.R. Maschek ¹¹², L. Masetti ⁹⁷, T. Mashimo ¹⁵⁹, J. Masik ⁹⁸, A.L. Maslennikov ^{118b,118a}, L. Massa ^{21b}, P. Massarotti ^{67a,67b}, P. Mastrandrea ^{69a,69b}, A. Mastroberardino ^{39b,39a}, T. Masubuchi ¹⁵⁹, D. Matakias ²⁷, T. Mathisen ¹⁶⁷, A. Matic ¹¹¹, N. Matsuzawa ¹⁵⁹, J. Maurer ^{25b}, B. Maček ⁸⁹, D.A. Maximov ^{118b,118a}, R. Mazini ¹⁵⁴, I. Maznas ¹⁵⁸, S.M. Mazza ¹⁴¹, C. Mc Ginn ²⁷, J.P. Mc Gowan ¹⁰¹, S.P. Mc Kee ¹⁰³, T.G. McCarthy ¹¹², W.P. McCormack ¹⁶, E.F. McDonald ¹⁰², A.E. McDougall ¹¹⁶, J.A. Mcfayden ¹⁵², G. Mchedlidze ^{155b}, M.A. McKay ⁴⁰, K.D. McLean ¹⁷¹, S.J. McMahon ¹³⁹, P.C. McNamara ¹⁰², R.A. McPherson ^{171,aa}, J.E. Mdhului ^{31f}, Z.A. Meadows ¹⁰⁰, S. Meehan ³⁴, T. Megy ³⁶, S. Mehlhase ¹¹¹, A. Mehta ⁸⁸, B. Meirose ⁴¹, D. Melini ¹⁵⁶, B.R. Mellado Garcia ^{31f}, F. Meloni ⁴⁴, A. Melzer ²², E.D. Mendes Gouveia ^{135a}, A.M. Mendes Jacques Da Costa ¹⁹, H.Y. Meng ¹⁶², L. Meng ³⁴, S. Menke ¹¹², M. Mentink ³⁴, E. Meoni ^{39b,39a}, C. Merlassino ¹³⁰, P. Mermod ^{52,*}, L. Merola ^{67a,67b}, C. Meroni ^{66a}, G. Merz ¹⁰³, O. Meshkov ^{110,108}, J.K.R. Meshreki ¹⁴⁷, J. Metcalfe ⁵, A.S. Mete ⁵, C. Meyer ⁶³, J.-P. Meyer ¹⁴⁰, M. Michetti ¹⁷, R.P. Middleton ¹³⁹, L. Mijović ⁴⁸, G. Mikenberg ¹⁷⁵, M. Mikestikova ¹³⁶, M. Mikuž ⁸⁹, H. Mildner ¹⁴⁵, A. Milic ¹⁶², C.D. Milke ⁴⁰, D.W. Miller ³⁵, L.S. Miller ³², A. Milov ¹⁷⁵, D.A. Milstead ^{43a,43b}, A.A. Minaenko ¹¹⁹, I.A. Minashvili ^{155b}, L. Mince ⁵⁵, A.I. Mincer ¹²¹, B. Mindur ^{81a}, M. Mineev ⁷⁷, Y. Minegishi ¹⁵⁹, Y. Mino ⁸³, L.M. Mir ¹², M. Miralles Lopez ¹⁶⁹, M. Mironova ¹³⁰, T. Mitani ¹⁷⁴, V.A. Mitsou ¹⁶⁹, M. Mittal ^{58c}, O. Miu ¹⁶², P.S. Miyagawa ⁹⁰, Y. Miyazaki ⁸⁵, A. Mizukami ⁷⁹, J.U. Mjörnmark ⁹⁴, T. Mkrtchyan ^{59a}, M. Mlynarikova ¹¹⁷, T. Moa ^{43a,43b}, S. Mobius ⁵¹, K. Mochizuki ¹⁰⁷, P. Moder ⁴⁴, P. Mogg ¹¹¹, A.F. Mohammed ^{13a}, S. Mohapatra ³⁷, G. Mokgatitswane ^{31f}, B. Mondal ¹⁴⁷, S. Mondal ¹³⁷, K. Mönig ⁴⁴, E. Monnier ⁹⁹, A. Montalbano ¹⁴⁸, J. Montejo Berlingen ³⁴, M. Montella ¹²³, F. Monticelli ⁸⁶, N. Morange ⁶², A.L. Moreira De Carvalho ^{135a}, M. Moreno Llácer ¹⁶⁹, C. Moreno Martinez ¹², P. Morettini ^{53b}, M. Morgenstern ¹⁵⁶, S. Morgenstern ¹⁷³, D. Mori ¹⁴⁸, M. Morii ⁵⁷, M. Morinaga ¹⁵⁹, V. Morisbak ¹²⁹, A.K. Morley ³⁴, A.P. Morris ⁹², L. Morvaj ³⁴, P. Moschovakos ³⁴, B. Moser ¹¹⁶, M. Mosidze ^{155b}, T. Moskalets ⁵⁰, P. Moskvitina ¹¹⁵, J. Moss ^{29,o}, E.J.W. Moyse ¹⁰⁰, S. Muanza ⁹⁹, J. Mueller ¹³⁴, R. Mueller ¹⁸, D. Muenstermann ⁸⁷, G.A. Mullier ⁹⁴, J.J. Mullin ¹³², D.P. Mungo ^{66a,66b}, J.L. Munoz Martinez ¹², F.J. Munoz Sanchez ⁹⁸, M. Murin ⁹⁸, P. Murin ^{26b}, W.J. Murray ^{173,139}, A. Murrone ^{66a,66b}, J.M. Muse ¹²⁴, M. Muškinja ¹⁶, C. Mwewa ²⁷, A.G. Myagkov ^{119,ag}, A.J. Myers ⁷, A.A. Myers ¹³⁴, G. Myers ⁶³, M. Myska ¹³⁷, B.P. Nachman ¹⁶, O. Nackenhorst ⁴⁵, A. Nag Nag ⁴⁶, K. Nagai ¹³⁰, K. Nagano ⁷⁹, J.L. Nagle ²⁷, E. Nagy ⁹⁹, A.M. Nairz ³⁴, Y. Nakahama ¹¹³, K. Nakamura ⁷⁹, H. Nanjo ¹²⁸, F. Napolitano ^{59a}, R. Narayan ⁴⁰, I. Naryshkin ¹³³, M. Naseri ³², C. Nass ²², T. Naumann ⁴⁴, G. Navarro ^{20a}, J. Navarro-Gonzalez ¹⁶⁹, R. Nayak ¹⁵⁷, P.Y. Nechaeva ¹⁰⁸, F. Nechansky ⁴⁴, T.J. Neep ¹⁹,

A. Negri^{68a,68b}, M. Negrini^{21b}, C. Nellist¹¹⁵, C. Nelson¹⁰¹, K. Nelson¹⁰³, M.E. Nelson^{43a,43b}, S. Nemecek¹³⁶, M. Nessi^{34,g}, M.S. Neubauer¹⁶⁸, F. Neuhaus⁹⁷, J. Neundorff⁴⁴, R. Newhouse¹⁷⁰, P.R. Newman¹⁹, C.W. Ng¹³⁴, Y.S. Ng¹⁷, Y.W.Y. Ng¹⁶⁶, B. Ngair^{33e}, H.D.N. Nguyen⁹⁹, R.B. Nickerson¹³⁰, R. Nicolaidou¹⁴⁰, D.S. Nielsen³⁸, J. Nielsen¹⁴¹, M. Niemeyer⁵¹, N. Nikiforou¹⁰, V. Nikolaenko^{119,ag}, I. Nikolic-Audit¹³¹, K. Nikolopoulos¹⁹, P. Nilsson²⁷, H.R. Nindhito⁵², A. Nisati^{70a}, N. Nishu², R. Nisius¹¹², T. Nitta¹⁷⁴, T. Nobe¹⁵⁹, D.L. Noel³⁰, Y. Noguchi⁸³, I. Nomidis¹³¹, M.A. Nomura²⁷, M.B. Norfolk¹⁴⁵, R.R.B. Norisam⁹², J. Novak⁸⁹, T. Novak⁴⁴, O. Novgorodova⁴⁶, L. Novotny¹³⁷, R. Novotny¹¹⁴, L. Nozka¹²⁶, K. Ntekas¹⁶⁶, E. Nurse⁹², F.G. Oakham^{32,al}, J. Ocariz¹³¹, A. Ochi⁸⁰, I. Ochoa^{135a}, J.P. Ochoa-Ricoux^{142a}, S. Oda⁸⁵, S. Odaka⁷⁹, S. Oerdek¹⁶⁷, A. Ogrodnik^{81a}, A. Oh⁹⁸, C.C. Ohm¹⁵⁰, H. Oide¹⁶⁰, R. Oishi¹⁵⁹, M.L. Ojeda¹⁶², Y. Okazaki⁸³, M.W. O’Keefe⁸⁸, Y. Okumura¹⁵⁹, A. Olariu^{25b}, L.F. Oleiro Seabra^{135a}, S.A. Olivares Pino^{142c}, D. Oliveira Damazio²⁷, D. Oliveira Goncalves^{78a}, J.L. Oliver¹⁶⁶, M.J.R. Olsson¹⁶⁶, A. Olszewski⁸², J. Olszowska⁸², Ö.O. Öncel²², D.C. O’Neil¹⁴⁸, A.P. O’neill¹³⁰, A. Onofre^{135a,135e}, P.U.E. Onyisi¹⁰, R.G. Oreamuno Madriz¹¹⁷, M.J. Oreglia³⁵, G.E. Orellana⁸⁶, D. Orestano^{72a,72b}, N. Orlando¹², R.S. Orr¹⁶², V. O’Shea⁵⁵, R. Ospanov^{58a}, G. Otero y Garzon²⁸, H. Otono⁸⁵, P.S. Ott^{59a}, G.J. Ottino¹⁶, M. Ouchrif^{33d}, J. Ouellette²⁷, F. Ould-Saada¹²⁹, A. Ouraou^{140,*}, Q. Ouyang^{13a}, M. Owen⁵⁵, R.E. Owen¹³⁹, K.Y. Oyulmaz^{11c}, V.E. Ozcan^{11c}, N. Ozturk⁷, S. Ozturk^{11c}, J. Pacalt¹²⁶, H.A. Pacey³⁰, K. Pachal⁴⁷, A. Pacheco Pages¹², C. Padilla Aranda¹², S. Pagan Griso¹⁶, G. Palacino⁶³, S. Palazzo⁴⁸, S. Palestini³⁴, M. Palka^{81b}, P. Palni^{81a}, D.K. Panchal¹⁰, C.E. Pandini⁵², J.G. Panduro Vazquez⁹¹, P. Pani⁴⁴, G. Panizzo^{64a,64c}, L. Paolozzi⁵², C. Papadatos¹⁰⁷, S. Parajuli⁴⁰, A. Paramonov⁵, C. Paraskevopoulos⁹, D. Paredes Hernandez^{60b}, S.R. Paredes Saenz¹³⁰, B. Parida¹⁷⁵, T.H. Park¹⁶², A.J. Parker²⁹, M.A. Parker³⁰, F. Parodi^{53b,53a}, E.W. Parrish¹¹⁷, J.A. Parsons³⁷, U. Parzefall⁵⁰, L. Pascual Dominguez¹⁵⁷, V.R. Pascuzzi¹⁶, F. Pasquali¹¹⁶, E. Pasqualucci^{70a}, S. Passaggio^{53b}, F. Pastore⁹¹, P. Pasuwan^{43a,43b}, J.R. Pater⁹⁸, A. Pathak¹⁷⁶, J. Patton⁸⁸, T. Pauly³⁴, J. Pearkes¹⁴⁹, M. Pedersen¹²⁹, L. Pedraza Diaz¹¹⁵, R. Pedro^{135a}, T. Peiffer⁵¹, S.V. Peleganchuk^{118b,118a}, O. Penc¹³⁶, C. Peng^{60b}, H. Peng^{58a}, M. Penzin¹⁶¹, B.S. Peralva^{78a}, M.M. Perego⁶², A.P. Pereira Peixoto^{135a}, L. Pereira Sanchez^{43a,43b}, D.V. Perepelitsa²⁷, E. Perez Codina^{163a}, M. Perganti⁹, L. Perini^{66a,66b}, H. Pernegger³⁴, S. Perrella³⁴, A. Perrevoort¹¹⁶, K. Peters⁴⁴, R.F.Y. Peters⁹⁸, B.A. Petersen³⁴, T.C. Petersen³⁸, E. Petit⁹⁹, V. Petousis¹³⁷, C. Petridou¹⁵⁸, P. Petroff⁶², F. Petrucci^{72a,72b}, M. Pettee¹⁷⁸, N.E. Pettersson³⁴, K. Petukhova¹³⁸, A. Peyaud¹⁴⁰, R. Pezoa^{142d}, L. Pezzotti^{68a,68b}, G. Pezzullo¹⁷⁸, T. Pham¹⁰², P.W. Phillips¹³⁹, M.W. Phipps¹⁶⁸, G. Piacquadio¹⁵¹, E. Pianori¹⁶, F. Piazza^{66a,66b}, A. Picazio¹⁰⁰, R. Piegai²⁸, D. Pietreanu^{25b}, J.E. Pilcher³⁵, A.D. Pilkington⁹⁸, M. Pinamonti^{64a,64c}, J.L. Pinfold², C. Pitman Donaldson⁹², D.A. Pizzi³², L. Pizzimento^{71a,71b}, A. Pizzini¹¹⁶, M.-A. Pleier²⁷, V. Plesanovs⁵⁰, V. Pleskot¹³⁸, E. Plotnikova⁷⁷, P. Podberezko^{118b,118a}, R. Poettgen⁹⁴, R. Poggi⁵², L. Poggioli¹³¹, I. Pogrebnyak¹⁰⁴, D. Pohl²², I. Pokharel⁵¹, G. Polesello^{68a}, A. Poley^{148,163a}, A. Policicchio^{70a,70b}, R. Polifka¹³⁸, A. Polini^{21b}, C.S. Pollard¹³⁰, Z.B. Pollock¹²³, V. Polychronakos²⁷, D. Ponomarenko¹⁰⁹, L. Pontecorvo³⁴, S. Popa^{25a}, G.A. Popeneciu^{25d}, L. Portales⁴, D.M. Portillo Quintero^{163a}, S. Pospisil¹³⁷, P. Postolache^{25c}, K. Potamianos¹³⁰, I.N. Potrap⁷⁷, C.J. Potter³⁰, H. Potti¹, T. Poulsen⁴⁴, J. Poveda¹⁶⁹, T.D. Powell¹⁴⁵, G. Pownall⁴⁴, M.E. Pozo Astigarraga³⁴, A. Prades Ibanez¹⁶⁹, P. Pralavorio⁹⁹, M.M. Prapa⁴², S. Prell⁷⁶, D. Price⁹⁸, M. Primavera^{65a}, M.A. Principe Martin⁹⁶, M.L. Proffitt¹⁴⁴, N. Proklova¹⁰⁹, K. Prokofiev^{60c}, F. Prokoshin⁷⁷, S. Protopopescu²⁷, J. Proudfoot⁵, M. Przybycien^{81a}, D. Pudzha¹³³, P. Puzo⁶², D. Pyatizbyantseva¹⁰⁹, J. Qian¹⁰³, Y. Qin⁹⁸, A. Quadt⁵¹, M. Queitsch-Maitland³⁴, G. Rabanal Bolanos⁵⁷, F. Ragusa^{66a,66b}, G. Rahal⁹⁵, J.A. Raine⁵², S. Rajagopalan²⁷, K. Ran^{13a,13d}, D.F. Rassloff^{59a}, D.M. Rauch⁴⁴, S. Rave⁹⁷, B. Ravina⁵⁵, I. Ravinovitch¹⁷⁵, M. Raymond³⁴, A.L. Read¹²⁹, N.P. Readioff¹⁴⁵, D.M. Rebuffi^{68a,68b}, G. Redlinger²⁷, K. Reeves⁴¹, D. Reikher¹⁵⁷, A. Reiss⁹⁷, A. Rej¹⁴⁷, C. Rembser³⁴, A. Renardi⁴⁴, M. Renda^{25b}, M.B. Rendel¹¹², A.G. Rennie⁵⁵, S. Resconi^{66a}, E.D. Resseguie¹⁶, S. Rettie⁹², B. Reynolds¹²³, E. Reynolds¹⁹, M. Rezaei Estabragh¹⁷⁷, O.L. Rezanova^{118b,118a}, P. Reznicek¹³⁸, E. Ricci^{73a,73b}, R. Richter¹¹², S. Richter⁴⁴, E. Richter-Was^{81b}, M. Ridel¹³¹, P. Rieck¹¹², P. Riedler³⁴, O. Rifki⁴⁴, M. Rijssenbeek¹⁵¹, A. Rimoldi^{68a,68b}, M. Rimoldi⁴⁴, L. Rinaldi^{21b,21a}, T.T. Rinn¹⁶⁸, M.P. Rinnagel¹¹¹, G. Ripellino¹⁵⁰, I. Riu¹², P. Rivadeneira⁴⁴, J.C. Rivera Vergara¹⁷¹, F. Rizatdinova¹²⁵, E. Rizvi⁹⁰, C. Rizzi⁵², B.A. Roberts¹⁷³, S.H. Robertson^{101,aa}, M. Robin⁴⁴, D. Robinson³⁰, C.M. Robles Gajardo^{142d}, M. Robles Manzano⁹⁷, A. Robson⁵⁵, A. Rocchi^{71a,71b}, C. Roda^{69a,69b}, S. Rodriguez Bosca^{59a}, A. Rodriguez Rodriguez⁵⁰, A.M. Rodríguez Vera^{163b}, S. Roe³⁴, A.R. Roepe¹²⁴,

J. Roggel¹⁷⁷, O. Røhne¹²⁹, R.A. Rojas^{142d}, B. Roland⁵⁰, C.P.A. Roland⁶³, J. Roloff²⁷, A. Romaniouk¹⁰⁹, M. Romano^{21b}, A.C. Romero Hernandez¹⁶⁸, N. Rompotis⁸⁸, M. Ronzani¹²¹, L. Roos¹³¹, S. Rosati^{70a}, G. Rosin¹⁰⁰, B.J. Rosser¹³², E. Rossi¹⁶², E. Rossi⁴, E. Rossi^{67a,67b}, L.P. Rossi^{53b}, L. Rossini⁴⁴, R. Rosten¹²³, M. Rotaru^{25b}, B. Rottler⁵⁰, D. Rousseau⁶², D. Rouso³⁰, G. Rovelli^{68a,68b}, A. Roy¹⁰, A. Rozanov⁹⁹, Y. Rozen¹⁵⁶, X. Ruan^{31f}, A.J. Ruby⁸⁸, T.A. Ruggeri¹, F. Rühr⁵⁰, A. Ruiz-Martinez¹⁶⁹, A. Rummler³⁴, Z. Rurikova⁵⁰, N.A. Rusakovich⁷⁷, H.L. Russell³⁴, L. Rustige³⁶, J.P. Rutherford⁶, E.M. Rüttinger¹⁴⁵, M. Rybar¹³⁸, E.B. Rye¹²⁹, A. Ryzhov¹¹⁹, J.A. Sabater Iglesias⁴⁴, P. Sabatini¹⁶⁹, L. Sabetta^{70a,70b}, H.F-W. Sadrozinski¹⁴¹, R. Sadykov⁷⁷, F. Safai Tehrani^{70a}, B. Safarzadeh Samani¹⁵², M. Safdari¹⁴⁹, P. Saha¹¹⁷, S. Saha¹⁰¹, M. Sahinsoy¹¹², A. Sahu¹⁷⁷, M. Saimpert¹⁴⁰, M. Saito¹⁵⁹, T. Saito¹⁵⁹, D. Salamani³⁴, G. Salamanna^{72a,72b}, A. Salnikov¹⁴⁹, J. Salt¹⁶⁹, A. Salvador Salas¹², D. Salvatore^{39b,39a}, F. Salvatore¹⁵², A. Salzburger³⁴, D. Sammel⁵⁰, D. Sampsonidis¹⁵⁸, D. Sampsonidou^{58d,58c}, J. Sánchez¹⁶⁹, A. Sanchez Pineda⁴, V. Sanchez Sebastian¹⁶⁹, H. Sandaker¹²⁹, C.O. Sander⁴⁴, I.G. Sanderswood⁸⁷, J.A. Sandesara¹⁰⁰, M. Sandhoff¹⁷⁷, C. Sandoval^{20b}, D.P.C. Sankey¹³⁹, M. Sannino^{53b,53a}, Y. Sano¹¹³, A. Sansoni⁴⁹, C. Santoni³⁶, H. Santos^{135a,135b}, S.N. Santpur¹⁶, A. Santra¹⁷⁵, K.A. Saoucha¹⁴⁵, A. Saproonov⁷⁷, J.G. Saraiva^{135a,135d}, J. Sardain⁹⁹, O. Sasaki⁷⁹, K. Sato¹⁶⁴, C. Sauer^{59b}, F. Sauerburger⁵⁰, E. Sauvan⁴, P. Savard^{162,al}, R. Sawada¹⁵⁹, C. Sawyer¹³⁹, L. Sawyer⁹³, I. Sayago Galvan¹⁶⁹, C. Sbarra^{21b}, A. Sbrizzi^{64a,64c}, T. Scanlon⁹², J. Schaarschmidt¹⁴⁴, P. Schacht¹¹², D. Schaefer³⁵, L. Schaefer¹³², U. Schäfer⁹⁷, A.C. Schaffer⁶², D. Schaile¹¹¹, R.D. Schamberger¹⁵¹, E. Schanet¹¹¹, C. Scharf¹⁷, N. Scharmberg⁹⁸, V.A. Schegelsky¹³³, D. Scheirich¹³⁸, F. Schenck¹⁷, M. Schernau¹⁶⁶, C. Schiavi^{53b,53a}, L.K. Schildgen²², Z.M. Schillaci²⁴, E.J. Schioppa^{65a,65b}, M. Schioppa^{39b,39a}, B. Schlag⁹⁷, K.E. Schleicher⁵⁰, S. Schlenker³⁴, K. Schmieden⁹⁷, C. Schmitt⁹⁷, S. Schmitt⁴⁴, L. Schoeffel¹⁴⁰, A. Schoening^{59b}, P.G. Scholer⁵⁰, E. Schopf¹³⁰, M. Schott⁹⁷, J. Schovancova³⁴, S. Schramm⁵², F. Schroeder¹⁷⁷, H-C. Schultz-Coulon^{59a}, M. Schumacher⁵⁰, B.A. Schumm¹⁴¹, Ph. Schune¹⁴⁰, A. Schwartzman¹⁴⁹, T.A. Schwarz¹⁰³, Ph. Schwemling¹⁴⁰, R. Schwienhorst¹⁰⁴, A. Sciandra¹⁴¹, G. Sciolla²⁴, F. Scuri^{69a}, F. Scutti¹⁰², C.D. Sebastiani⁸⁸, K. Sedlaczek⁴⁵, P. Seema¹⁷, S.C. Seidel¹¹⁴, A. Seiden¹⁴¹, B.D. Seidlitz²⁷, T. Seiss³⁵, C. Seitz⁴⁴, J.M. Seixas^{78b}, G. Sekhniaidze^{67a}, S.J. Sekula⁴⁰, L. Selem⁴, N. Semprini-Cesari^{21b,21a}, S. Sen⁴⁷, C. Serfon²⁷, L. Serin⁶², L. Serkin^{64a,64b}, M. Sessa^{58a}, H. Severini¹²⁴, S. Sevova¹⁴⁹, F. Sforza^{53b,53a}, A. Sfyrla⁵², E. Shabalina⁵¹, R. Shaheen¹⁵⁰, J.D. Shahinian¹³², N.W. Shaikh^{43a,43b}, D. Shaked Renous¹⁷⁵, L.Y. Shan^{13a}, M. Shapiro¹⁶, A. Sharma³⁴, A.S. Sharma¹, S. Sharma⁴⁴, P.B. Shatalov¹²⁰, K. Shaw¹⁵², S.M. Shaw⁹⁸, P. Sherwood⁹², L. Shi⁹², C.O. Shimmin¹⁷⁸, Y. Shimogama¹⁷⁴, J.D. Shinner⁹¹, I.P.J. Shipsey¹³⁰, S. Shirabe⁵², M. Shiyakova⁷⁷, J. Shlomi¹⁷⁵, M.J. Shochet³⁵, J. Shojaii¹⁰², D.R. Shope¹⁵⁰, S. Shrestha¹²³, E.M. Shrif^{31f}, M.J. Shroff¹⁷¹, E. Shulga¹⁷⁵, P. Sicho¹³⁶, A.M. Sickles¹⁶⁸, E. Sideras Haddad^{31f}, O. Sidiropoulou³⁴, A. Sidoti^{21b}, F. Siegert⁴⁶, Dj. Sijacki¹⁴, J.M. Silva¹⁹, M.V. Silva Oliveira³⁴, S.B. Silverstein^{43a}, S. Simion⁶², R. Simoniello³⁴, S. Simsek^{11b}, P. Sinervo¹⁶², V. Sinetckii¹¹⁰, S. Singh¹⁴⁸, S. Sinha⁴⁴, S. Sinha^{31f}, M. Sioli^{21b,21a}, I. Siral¹²⁷, S.Yu. Sivoklov¹¹⁰, J. Sjölin^{43a,43b}, A. Skaf⁵¹, E. Skorda⁹⁴, P. Skubic¹²⁴, M. Slawinska⁸², K. Sliwa¹⁶⁵, V. Smakhtin¹⁷⁵, B.H. Smart¹³⁹, J. Smiesko¹³⁸, S.Yu. Smirnov¹⁰⁹, Y. Smirnov¹⁰⁹, L.N. Smirnova^{110,s}, O. Smirnova⁹⁴, E.A. Smith³⁵, H.A. Smith¹³⁰, M. Smizanska⁸⁷, K. Smolek¹³⁷, A. Smykiewicz⁸², A.A. Snesarev¹⁰⁸, H.L. Snoek¹¹⁶, S. Snyder²⁷, R. Sobie^{171,aa}, A. Soffer¹⁵⁷, F. Sohns⁵¹, C.A. Solans Sanchez³⁴, E.Yu. Soldatov¹⁰⁹, U. Soldevila¹⁶⁹, A.A. Solodkov¹¹⁹, S. Solomon⁵⁰, A. Soloshenko⁷⁷, O.V. Solovyanov¹¹⁹, V. Solovyev¹³³, P. Sommer¹⁴⁵, H. Son¹⁶⁵, A. Sonay¹², W.Y. Song^{163b}, A. Sopczak¹³⁷, A.L. Sopio⁹², F. Sopkova^{26b}, S. Sottocornola^{68a,68b}, R. Soualah^{64a,64c}, A.M. Soukharev^{118b,118a}, Z. Soumami^{33e}, D. South⁴⁴, S. Spagnolo^{65a,65b}, M. Spalla¹¹², M. Spangenberg¹⁷³, F. Spanò⁹¹, D. Sperlich⁵⁰, T.M. Spieker^{59a}, G. Spigo³⁴, M. Spina¹⁵², D.P. Spiteri⁵⁵, M. Spousta¹³⁸, A. Stabile^{66a,66b}, R. Stamen^{59a}, M. Stamenkovic¹¹⁶, A. Stampekis¹⁹, M. Standke²², E. Stanecka⁸², B. Stanislaus³⁴, M.M. Stanitzki⁴⁴, M. Stankaityte¹³⁰, B. Stapf⁴⁴, E.A. Starchenko¹¹⁹, G.H. Stark¹⁴¹, J. Stark⁹⁹, D.M. Starke^{163b}, P. Staroba¹³⁶, P. Starovoitov^{59a}, S. Stärz¹⁰¹, R. Staszewski⁸², G. Stavropoulos⁴², P. Steinberg²⁷, A.L. Steinhebel¹²⁷, B. Stelzer^{148,163a}, H.J. Stelzer¹³⁴, O. Stelzer-Chilton^{163a}, H. Stenzel⁵⁴, T.J. Stevenson¹⁵², G.A. Stewart³⁴, M.C. Stockton³⁴, G. Stoica^{25b}, M. Stolarski^{135a}, S. Stonjek¹¹², A. Straessner⁴⁶, J. Strandberg¹⁵⁰, S. Strandberg^{43a,43b}, M. Strauss¹²⁴, T. Strebler⁹⁹, P. Strizenec^{26b}, R. Ströhmer¹⁷², D.M. Strom¹²⁷, L.R. Strom⁴⁴, R. Stroynowski⁴⁰, A. Strubig^{43a,43b}, S.A. Stucci²⁷, B. Stugu¹⁵, J. Stupak¹²⁴, N.A. Styles⁴⁴, D. Su¹⁴⁹, S. Su^{58a}, W. Su^{58d,144,58c}, X. Su^{58a}, N.B. Suarez¹³⁴, K. Sugizaki¹⁵⁹, V.V. Sulin¹⁰⁸, M.J. Sullivan⁸⁸, D.M.S. Sultan⁵²,

S. Sultansoy^{3c}, T. Sumida⁸³, S. Sun¹⁰³, S. Sun¹⁷⁶, X. Sun⁹⁸, O. Sunneborn Gudnadottir¹⁶⁷, C.J.E. Suster¹⁵³, M.R. Sutton¹⁵², M. Svatos¹³⁶, M. Swiatlowski^{163a}, T. Swirski¹⁷², I. Sykora^{26a}, M. Sykora¹³⁸, T. Sykora¹³⁸, D. Ta⁹⁷, K. Tackmann^{44,y}, A. Taffard¹⁶⁶, R. Tafirout^{163a}, E. Tagiev¹¹⁹, R.H.M. Taibah¹³¹, R. Takashima⁸⁴, K. Takeda⁸⁰, T. Takeshita¹⁴⁶, E.P. Takeva⁴⁸, Y. Takubo⁷⁹, M. Talby⁹⁹, A.A. Talyshev^{118b,118a}, K.C. Tam^{60b}, N.M. Tamir¹⁵⁷, A. Tanaka¹⁵⁹, J. Tanaka¹⁵⁹, R. Tanaka⁶², Z. Tao¹⁷⁰, S. Tapia Araya⁷⁶, S. Tapprogge⁹⁷, A. Tarek Abouelfadl Mohamed¹⁰⁴, S. Tarem¹⁵⁶, K. Tariq^{58b}, G. Tarna^{25b,f}, G.F. Tartarelli^{66a}, P. Tas¹³⁸, M. Tasevsky¹³⁶, E. Tassi^{39b,39a}, G. Tateno¹⁵⁹, Y. Tayalati^{33e}, G.N. Taylor¹⁰², W. Taylor^{163b}, H. Teagle⁸⁸, A.S. Tee¹⁷⁶, R. Teixeira De Lima¹⁴⁹, P. Teixeira-Dias⁹¹, H. Ten Kate³⁴, J.J. Teoh¹¹⁶, K. Terashi¹⁵⁹, J. Terron⁹⁶, S. Terzo¹², M. Testa⁴⁹, R.J. Teuscher^{162,aa}, N. Themistokleous⁴⁸, T. Theveneaux-Pelzer¹⁷, O. Thielmann¹⁷⁷, D.W. Thomas⁹¹, J.P. Thomas¹⁹, E.A. Thompson⁴⁴, P.D. Thompson¹⁹, E. Thomson¹³², E.J. Thorpe⁹⁰, Y. Tian⁵¹, V.O. Tikhomirov^{108,ah}, Yu.A. Tikhonov^{118b,118a}, S. Timoshenko¹⁰⁹, P. Tipton¹⁷⁸, S. Tisserant⁹⁹, S.H. Tlou^{31f}, A. Tmourji³⁶, K. Todome^{21b,21a}, S. Todorova-Nova¹³⁸, S. Todt⁴⁶, M. Togawa⁷⁹, J. Tojo⁸⁵, S. Tokár^{26a}, K. Tokushuku⁷⁹, E. Tolley¹²³, R. Tombs³⁰, M. Tomoto^{79,113}, L. Tompkins¹⁴⁹, P. Tornambe¹⁰⁰, E. Torrence¹²⁷, H. Torres⁴⁶, E. Torró Pastor¹⁶⁹, M. Toscani²⁸, C. Tosciri³⁵, J. Toth^{99,z}, D.R. Tovey¹⁴⁵, A. Traet¹⁵, C.J. Treado¹²¹, T. Trefzger¹⁷², A. Tricoli²⁷, I.M. Trigger^{163a}, S. Trincaz-Duvoid¹³¹, D.A. Trischuk¹⁷⁰, W. Trischuk¹⁶², B. Trocmé⁵⁶, A. Trofymov⁶², C. Troncon^{66a}, F. Trovato¹⁵², L. Truong^{31c}, M. Trzebinski⁸², A. Trzupek⁸², F. Tsai¹⁵¹, A. Tsiamis¹⁵⁸, P.V. Tsiarehshka^{105,af}, A. Tsirigotis^{158,w}, V. Tsiskaridze¹⁵¹, E.G. Tskhadadze^{155a}, M. Tsopoulou¹⁵⁸, I.I. Tsukerman¹²⁰, V. Tsulaia¹⁶, S. Tsuno⁷⁹, O. Tsur¹⁵⁶, D. Tsybychev¹⁵¹, Y. Tu^{60b}, A. Tudorache^{25b}, V. Tudorache^{25b}, A.N. Tuna³⁴, S. Turchikhin⁷⁷, I. Turk Cakir^{3b,u}, R.J. Turner¹⁹, R. Turra^{66a}, P.M. Tuts³⁷, S. Tzamarias¹⁵⁸, P. Tzani⁹, E. Tzovara⁹⁷, K. Uchida¹⁵⁹, F. Ukegawa¹⁶⁴, G. Unal³⁴, M. Unal¹⁰, A. Undrus²⁷, G. Unel¹⁶⁶, F.C. Ungaro¹⁰², K. Uno¹⁵⁹, J. Urban^{26b}, P. Urquijo¹⁰², G. Usai⁷, R. Ushioda¹⁶⁰, M. Usman¹⁰⁷, Z. Uysal^{11d}, V. Vacek¹³⁷, B. Vachon¹⁰¹, K.O.H. Vadla¹²⁹, T. Vafeiadis³⁴, C. Valderanis¹¹¹, E. Valdes Santurio^{43a,43b}, M. Valente^{163a}, S. Valentinetti^{21b,21a}, A. Valero¹⁶⁹, L. Valéry⁴⁴, R.A. Vallance¹⁹, A. Vallier⁹⁹, J.A. Valls Ferrer¹⁶⁹, T.R. Van Daalen¹⁴⁴, P. Van Gemmeren⁵, S. Van Stroud⁹², I. Van Vulpen¹¹⁶, M. Vanadia^{71a,71b}, W. Vandelli³⁴, M. Vandenbroucke¹⁴⁰, E.R. Vandewall¹²⁵, D. Vannicola¹⁵⁷, L. Vannoli^{53b,53a}, R. Vari^{70a}, E.W. Varnes⁶, C. Varni¹⁶, T. Varol¹⁵⁴, D. Varouchas⁶², K.E. Varvell¹⁵³, M.E. Vasile^{25b}, L. Vaslin³⁶, G.A. Vasquez¹⁷¹, F. Vazeille³⁶, D. Vazquez Furelos¹², T. Vazquez Schroeder³⁴, J. Veatch⁵¹, V. Vecchio⁹⁸, M.J. Veen¹¹⁶, I. Veliscek¹³⁰, L.M. Veloce¹⁶², F. Veloso^{135a,135c}, S. Veneziano^{70a}, A. Ventura^{65a,65b}, A. Verbytskyi¹¹², M. Verducci^{69a,69b}, C. Vergis²², M. Verissimo De Araujo^{78b}, W. Verkerke¹¹⁶, A.T. Vermeulen¹¹⁶, J.C. Vermeulen¹¹⁶, C. Vernieri¹⁴⁹, P.J. Verschuur⁹¹, M.L. Vesterbacka¹²¹, M.C. Vetterli^{148,al}, A. Vgenopoulos¹⁵⁸, N. Viaux Maira^{142d}, T. Vickey¹⁴⁵, O.E. Vickey Boeriu¹⁴⁵, G.H.A. Viehhauser¹³⁰, L. Vigani^{59b}, M. Villa^{21b,21a}, M. Villaplana Perez¹⁶⁹, E.M. Villhauer⁴⁸, E. Vilucchi⁴⁹, M.G. Vincker³², G.S. Virdee¹⁹, A. Vishwakarma⁴⁸, C. Vittori^{21b,21a}, I. Vivarelli¹⁵², V. Vladimirov¹⁷³, E. Voevodina¹¹², M. Vogel¹⁷⁷, P. Vokac¹³⁷, J. Von Ahnen⁴⁴, S.E. von Buddenbrock^{31f}, E. Von Toerne²², V. Vorobel¹³⁸, K. Vorobev¹⁰⁹, M. Vos¹⁶⁹, J.H. Vosseveld⁸⁸, M. Vozak⁹⁸, L. Vozdecky⁹⁰, N. Vranjes¹⁴, M. Vranjes Milosavljevic¹⁴, V. Vrba^{137,*}, M. Vreeswijk¹¹⁶, N.K. Vu⁹⁹, R. Vuillermet³⁴, I. Vukotic³⁵, S. Wada¹⁶⁴, C. Wagner¹⁰⁰, P. Wagner²², W. Wagner¹⁷⁷, S. Wahdan¹⁷⁷, H. Wahlberg⁸⁶, R. Wakasa¹⁶⁴, M. Wakida¹¹³, V.M. Walbrecht¹¹², J. Walder¹³⁹, R. Walker¹¹¹, S.D. Walker⁹¹, W. Walkowiak¹⁴⁷, A.M. Wang⁵⁷, A.Z. Wang¹⁷⁶, C. Wang^{58a}, C. Wang^{58c}, H. Wang¹⁶, J. Wang^{60a}, P. Wang⁴⁰, R.-J. Wang⁹⁷, R. Wang⁵⁷, R. Wang¹¹⁷, S.M. Wang¹⁵⁴, S. Wang^{58b}, T. Wang^{58a}, W.T. Wang^{58a}, W.X. Wang^{58a}, X. Wang^{13c}, X. Wang¹⁶⁸, Y. Wang^{58a}, Z. Wang¹⁰³, C. Wanotayaroj³⁴, A. Warburton¹⁰¹, C.P. Ward³⁰, R.J. Ward¹⁹, N. Warrack⁵⁵, A.T. Watson¹⁹, M.F. Watson¹⁹, G. Watts¹⁴⁴, B.M. Waugh⁹², A.F. Webb¹⁰, C. Weber²⁷, M.S. Weber¹⁸, S.A. Weber³², S.M. Weber^{59a}, C. Wei^{58a}, Y. Wei¹³⁰, A.R. Weidberg¹³⁰, J. Weingarten⁴⁵, M. Weirich⁹⁷, C. Weiser⁵⁰, T. Wenaus²⁷, B. Wendland⁴⁵, T. Wengler³⁴, S. Wenig³⁴, N. Wermes²², M. Wessels^{59a}, K. Whalen¹²⁷, A.M. Wharton⁸⁷, A.S. White⁵⁷, A. White⁷, M.J. White¹, D. Whiteson¹⁶⁶, L. Wickremasinghe¹²⁸, W. Wiedenmann¹⁷⁶, C. Wiel⁴⁶, M. Wielers¹³⁹, N. Wieseotte⁹⁷, C. Wiglesworth³⁸, L.A.M. Wiik-Fuchs⁵⁰, D.J. Wilbern¹²⁴, H.G. Wilkens³⁴, L.J. Wilkins⁹¹, D.M. Williams³⁷, H.H. Williams¹³², S. Williams³⁰, S. Willocq¹⁰⁰, P.J. Windischhofer¹³⁰, I. Wingerter-Seez⁴, F. Winklmeier¹²⁷, B.T. Winter⁵⁰, M. Wittgen¹⁴⁹, M. Wobisch⁹³, A. Wolf⁹⁷, R. Wölker¹³⁰, J. Wollrath¹⁶⁶, M.W. Wolter⁸², H. Wolters^{135a,135c}, V.W.S. Wong¹⁷⁰, A.F. Wongel⁴⁴, S.D. Worm⁴⁴, B.K. Wosiek⁸², K.W. Woźniak⁸², K. Wraight⁵⁵, J. Wu^{13a,13d}, S.L. Wu¹⁷⁶, X. Wu⁵²,

Y. Wu^{58a}, Z. Wu^{140,58a}, J. Wuerzinger¹³⁰, T.R. Wyatt⁹⁸, B.M. Wynne⁴⁸, S. Xella³⁸, J. Xiang^{60c}, X. Xiao¹⁰³, M. Xie^{58a}, X. Xie^{58a}, I. Xiolidis¹⁵², D. Xu^{13a}, H. Xu^{58a}, H. Xu^{58a}, L. Xu^{58a}, R. Xu¹³², T. Xu^{58a}, W. Xu¹⁰³, Y. Xu^{13b}, Z. Xu^{58b}, Z. Xu¹⁴⁹, B. Yabsley¹⁵³, S. Yacoob^{31a}, N. Yamaguchi⁸⁵, Y. Yamaguchi¹⁶⁰, M. Yamatani¹⁵⁹, H. Yamauchi¹⁶⁴, T. Yamazaki¹⁶, Y. Yamazaki⁸⁰, J. Yan^{58c}, S. Yan¹³⁰, Z. Yan²³, H.J. Yang^{58c,58d}, H.T. Yang¹⁶, S. Yang^{58a}, T. Yang^{60c}, X. Yang^{58a}, X. Yang^{13a}, Y. Yang¹⁵⁹, Z. Yang^{103,58a}, W.-M. Yao¹⁶, Y.C. Yap⁴⁴, H. Ye^{13c}, J. Ye⁴⁰, S. Ye²⁷, I. Yeletsikh⁷⁷, M.R. Yexley⁸⁷, P. Yin³⁷, K. Yorita¹⁷⁴, K. Yoshihara⁷⁶, C.J.S. Young⁵⁰, C. Young¹⁴⁹, R. Yuan^{58b,j}, X. Yue^{59a}, M. Zaazoua^{33e}, B. Zabinski⁸², G. Zacharis⁹, E. Zaffaroni⁵², E. Zaid⁴⁸, A.M. Zaitsev^{119,ag}, T. Zakareishvili^{155b}, N. Zakharchuk³², S. Zambito³⁴, D. Zanzi⁵⁰, S.V. Zeißner⁴⁵, C. Zeitnitz¹⁷⁷, G. Zemaityte¹³⁰, J.C. Zeng¹⁶⁸, O. Zenin¹¹⁹, T. Ženiš^{26a}, S. Zenz⁹⁰, S. Zerradi^{33a}, D. Zerwas⁶², M. Zgubič¹³⁰, B. Zhang^{13c}, D.F. Zhang^{13b}, G. Zhang^{13b}, J. Zhang⁵, K. Zhang^{13a}, L. Zhang^{13c}, M. Zhang¹⁶⁸, R. Zhang¹⁷⁶, S. Zhang¹⁰³, X. Zhang^{58c}, X. Zhang^{58b}, Z. Zhang⁶², P. Zhao⁴⁷, Y. Zhao¹⁴¹, Z. Zhao^{58a}, A. Zhemchugov⁷⁷, Z. Zheng¹⁴⁹, D. Zhong¹⁶⁸, B. Zhou¹⁰³, C. Zhou¹⁷⁶, H. Zhou⁶, N. Zhou^{58c}, Y. Zhou⁶, C.G. Zhu^{58b}, C. Zhu^{13a,13d}, H.L. Zhu^{58a}, H. Zhu^{13a}, J. Zhu¹⁰³, Y. Zhu^{58a}, X. Zhuang^{13a}, K. Zhukov¹⁰⁸, V. Zhulanov^{118b,118a}, D. Zieminska⁶³, N.I. Zimine⁷⁷, S. Zimmermann^{50,*}, M. Ziolkowski¹⁴⁷, L. Živković¹⁴, A. Zoccoli^{21b,21a}, K. Zoch⁵², T.G. Zorbas¹⁴⁵, O. Zormpa⁴², W. Zou³⁷, L. Zwalinski³⁴

¹ Department of Physics, University of Adelaide, Adelaide; Australia

² Department of Physics, University of Alberta, Edmonton AB; Canada

³ (a) Department of Physics, Ankara University, Ankara; (b) Istanbul Aydın University, Application and Research Center for Advanced Studies, Istanbul; (c) Division of Physics, TOBB University of Economics and Technology, Ankara; Turkey

⁴ LAPP, Univ. Savoie Mont Blanc, CNRS/IN2P3, Annecy; France

⁵ High Energy Physics Division, Argonne National Laboratory, Argonne IL; United States of America

⁶ Department of Physics, University of Arizona, Tucson AZ; United States of America

⁷ Department of Physics, University of Texas at Arlington, Arlington TX; United States of America

⁸ Physics Department, National and Kapodistrian University of Athens, Athens; Greece

⁹ Physics Department, National Technical University of Athens, Zografou; Greece

¹⁰ Department of Physics, University of Texas at Austin, Austin TX; United States of America

¹¹ (a) Bahcesehir University, Faculty of Engineering and Natural Sciences, Istanbul; (b) Istanbul Bilgi University, Faculty of Engineering and Natural Sciences, Istanbul; (c) Department of Physics, Bogazici University, Istanbul; (d) Department of Physics Engineering, Gaziantep University, Gaziantep; Turkey

¹² Institut de Física d'Altes Energies (IFAE), Barcelona Institute of Science and Technology, Barcelona; Spain

¹³ (a) Institute of High Energy Physics, Chinese Academy of Sciences, Beijing; (b) Physics Department, Tsinghua University, Beijing; (c) Department of Physics, Nanjing University, Nanjing;

(d) University of Chinese Academy of Science (UCAS), Beijing; China

¹⁴ Institute of Physics, University of Belgrade, Belgrade; Serbia

¹⁵ Department for Physics and Technology, University of Bergen, Bergen; Norway

¹⁶ Physics Division, Lawrence Berkeley National Laboratory and University of California, Berkeley CA; United States of America

¹⁷ Institut für Physik, Humboldt Universität zu Berlin, Berlin; Germany

¹⁸ Albert Einstein Center for Fundamental Physics and Laboratory for High Energy Physics, University of Bern, Bern; Switzerland

¹⁹ School of Physics and Astronomy, University of Birmingham, Birmingham; United Kingdom

²⁰ (a) Facultad de Ciencias y Centro de Investigaciones, Universidad Antonio Nariño, Bogotá; (b) Departamento de Física, Universidad Nacional de Colombia, Bogotá; Colombia

²¹ (a) Dipartimento di Fisica e Astronomia A. Righi, Università di Bologna, Bologna; (b) INFN Sezione di Bologna; Italy

²² Physikalisches Institut, Universität Bonn, Bonn; Germany

²³ Department of Physics, Boston University, Boston MA; United States of America

²⁴ Department of Physics, Brandeis University, Waltham MA; United States of America

²⁵ (a) Transilvania University of Brasov, Brasov; (b) Horia Hulubei National Institute of Physics and Nuclear Engineering, Bucharest; (c) Department of Physics, Alexandru Ioan Cuza University of Iasi, Iasi; (d) National Institute for Research and Development of Isotopic and Molecular Technologies, Physics Department, Cluj-Napoca; (e) University Politehnica Bucharest, Bucharest; (f) West University in Timisoara, Timisoara; Romania

²⁶ (a) Faculty of Mathematics, Physics and Informatics, Comenius University, Bratislava; (b) Department of Subnuclear Physics, Institute of Experimental Physics of the Slovak Academy of Sciences, Kosice; Slovak Republic

²⁷ Physics Department, Brookhaven National Laboratory, Upton NY; United States of America

²⁸ Departamento de Física (FCEN) and IFIBA, Universidad de Buenos Aires and CONICET, Buenos Aires; Argentina

²⁹ California State University, CA; United States of America

³⁰ Cavendish Laboratory, University of Cambridge, Cambridge; United Kingdom

³¹ (a) Department of Physics, University of Cape Town, Cape Town; (b) iThemba Labs, Western Cape; (c) Department of Mechanical Engineering Science, University of Johannesburg, Johannesburg; (d) National Institute of Physics, University of the Philippines Diliman (Philippines); (e) University of South Africa, Department of Physics, Pretoria; (f) School of Physics, University of the Witwatersrand, Johannesburg; South Africa

³² Department of Physics, Carleton University, Ottawa ON; Canada

³³ (a) Faculté des Sciences Ain Chock, Réseau Universitaire de Physique des Hautes Energies – Université Hassan II, Casablanca; (b) Faculté des Sciences, Université Ibn-Tofail, Kénitra;

(c) Faculté des Sciences Semlalia, Université Cadi Ayyad, LPHEA, Marrakech; (d) LPMR, Faculté des Sciences, Université Mohamed Premier, Oujda; (e) Faculté des sciences, Université Mohammed V, Rabat; Morocco

³⁴ CERN, Geneva; Switzerland

³⁵ Enrico Fermi Institute, University of Chicago, Chicago IL; United States of America

³⁶ LPC, Université Clermont Auvergne, CNRS/IN2P3, Clermont-Ferrand; France

³⁷ Nevis Laboratory, Columbia University, Irvington NY; United States of America

³⁸ Niels Bohr Institute, University of Copenhagen, Copenhagen; Denmark

³⁹ (a) Dipartimento di Fisica, Università della Calabria, Rende; (b) INFN Gruppo Collegato di Cosenza, Laboratori Nazionali di Frascati; Italy

⁴⁰ Physics Department, Southern Methodist University, Dallas TX; United States of America

⁴¹ Physics Department, University of Texas at Dallas, Richardson TX; United States of America

⁴² National Centre for Scientific Research "Demokritos", Agia Paraskevi; Greece

⁴³ (a) Department of Physics, Stockholm University; (b) Oskar Klein Centre, Stockholm; Sweden

⁴⁴ Deutsches Elektronen-Synchrotron DESY, Hamburg and Zeuthen; Germany

⁴⁵ Fakultät Physik, Technische Universität Dortmund, Dortmund; Germany

- ⁴⁶ Institut für Kern- und Teilchenphysik, Technische Universität Dresden, Dresden; Germany
- ⁴⁷ Department of Physics, Duke University, Durham NC; United States of America
- ⁴⁸ SUPA – School of Physics and Astronomy, University of Edinburgh, Edinburgh; United Kingdom
- ⁴⁹ INFN e Laboratori Nazionali di Frascati, Frascati; Italy
- ⁵⁰ Physikalisches Institut, Albert-Ludwigs-Universität Freiburg, Freiburg; Germany
- ⁵¹ II. Physikalisches Institut, Georg-August-Universität Göttingen, Göttingen; Germany
- ⁵² Département de Physique Nucléaire et Corpusculaire, Université de Genève, Genève; Switzerland
- ⁵³ ^(a) Dipartimento di Fisica, Università di Genova, Genova; ^(b) INFN Sezione di Genova; Italy
- ⁵⁴ II. Physikalisches Institut, Justus-Liebig-Universität Giessen, Giessen; Germany
- ⁵⁵ SUPA – School of Physics and Astronomy, University of Glasgow, Glasgow; United Kingdom
- ⁵⁶ LPCS, Université Grenoble Alpes, CNRS/IN2P3, Grenoble INP, Grenoble; France
- ⁵⁷ Laboratory for Particle Physics and Cosmology, Harvard University, Cambridge MA; United States of America
- ⁵⁸ ^(a) Department of Modern Physics and State Key Laboratory of Particle Detection and Electronics, University of Science and Technology of China, Hefei; ^(b) Institute of Frontier and Interdisciplinary Science and Key Laboratory of Particle Physics and Particle Irradiation (MOE), Shandong University, Qingdao; ^(c) School of Physics and Astronomy, Shanghai Jiao Tong University, Key Laboratory for Particle Astrophysics and Cosmology (MOE), SKLPPC, Shanghai; ^(d) Tsung-Dao Lee Institute, Shanghai; China
- ⁵⁹ ^(a) Kirchhoff-Institut für Physik, Ruprecht-Karls-Universität Heidelberg, Heidelberg; ^(b) Physikalisches Institut, Ruprecht-Karls-Universität Heidelberg, Heidelberg; Germany
- ⁶⁰ ^(a) Department of Physics, Chinese University of Hong Kong, Shatin, N.T., Hong Kong; ^(b) Department of Physics, University of Hong Kong, Hong Kong; ^(c) Department of Physics and Institute for Advanced Study, Hong Kong University of Science and Technology, Clear Water Bay, Kowloon, Hong Kong; China
- ⁶¹ Department of Physics, National Tsing Hua University, Hsinchu; Taiwan
- ⁶² IJCLab, Université Paris-Saclay, CNRS/IN2P3, 91405, Orsay; France
- ⁶³ Department of Physics, Indiana University, Bloomington IN; United States of America
- ⁶⁴ ^(a) INFN Gruppo Collegato di Udine, Sezione di Trieste, Udine; ^(b) ICTP, Trieste; ^(c) Dipartimento Politecnico di Ingegneria e Architettura, Università di Udine, Udine; Italy
- ⁶⁵ ^(a) INFN Sezione di Lecce; ^(b) Dipartimento di Matematica e Fisica, Università del Salento, Lecce; Italy
- ⁶⁶ ^(a) INFN Sezione di Milano; ^(b) Dipartimento di Fisica, Università di Milano, Milano; Italy
- ⁶⁷ ^(a) INFN Sezione di Napoli; ^(b) Dipartimento di Fisica, Università di Napoli, Napoli; Italy
- ⁶⁸ ^(a) INFN Sezione di Pavia; ^(b) Dipartimento di Fisica, Università di Pavia, Pavia; Italy
- ⁶⁹ ^(a) INFN Sezione di Pisa; ^(b) Dipartimento di Fisica E. Fermi, Università di Pisa, Pisa; Italy
- ⁷⁰ ^(a) INFN Sezione di Roma; ^(b) Dipartimento di Fisica, Sapienza Università di Roma, Roma; Italy
- ⁷¹ ^(a) INFN Sezione di Roma Tor Vergata; ^(b) Dipartimento di Fisica, Università di Roma Tor Vergata, Roma; Italy
- ⁷² ^(a) INFN Sezione di Roma Tre; ^(b) Dipartimento di Matematica e Fisica, Università Roma Tre, Roma; Italy
- ⁷³ ^(a) INFN-TIFPA; ^(b) Università degli Studi di Trento, Trento; Italy
- ⁷⁴ Institut für Astro- und Teilchenphysik, Leopold-Franzens-Universität, Innsbruck; Austria
- ⁷⁵ University of Iowa, Iowa City IA; United States of America
- ⁷⁶ Department of Physics and Astronomy, Iowa State University, Ames IA; United States of America
- ⁷⁷ Joint Institute for Nuclear Research, Dubna; Russia
- ⁷⁸ ^(a) Departamento de Engenharia Elétrica, Universidade Federal de Juiz de Fora (UFJF), Juiz de Fora; ^(b) Universidade Federal do Rio De Janeiro COPPE/EE/IF, Rio de Janeiro; ^(c) Instituto de Física, Universidade de São Paulo, São Paulo; Brazil
- ⁷⁹ KEK, High Energy Accelerator Research Organization, Tsukuba; Japan
- ⁸⁰ Graduate School of Science, Kobe University, Kobe; Japan
- ⁸¹ ^(a) AGH University of Science and Technology, Faculty of Physics and Applied Computer Science, Krakow; ^(b) Marian Smoluchowski Institute of Physics, Jagiellonian University, Krakow; Poland
- ⁸² Institute of Nuclear Physics Polish Academy of Sciences, Krakow; Poland
- ⁸³ Faculty of Science, Kyoto University, Kyoto; Japan
- ⁸⁴ Kyoto University of Education, Kyoto; Japan
- ⁸⁵ Research Center for Advanced Particle Physics and Department of Physics, Kyushu University, Fukuoka; Japan
- ⁸⁶ Instituto de Física La Plata, Universidad Nacional de La Plata and CONICET, La Plata; Argentina
- ⁸⁷ Physics Department, Lancaster University, Lancaster; United Kingdom
- ⁸⁸ Oliver Lodge Laboratory, University of Liverpool, Liverpool; United Kingdom
- ⁸⁹ Department of Experimental Particle Physics, Jožef Stefan Institute and Department of Physics, University of Ljubljana, Ljubljana; Slovenia
- ⁹⁰ School of Physics and Astronomy, Queen Mary University of London, London; United Kingdom
- ⁹¹ Department of Physics, Royal Holloway University of London, Egham; United Kingdom
- ⁹² Department of Physics and Astronomy, University College London, London; United Kingdom
- ⁹³ Louisiana Tech University, Ruston LA; United States of America
- ⁹⁴ Fysiska institutionen, Lunds universitet, Lund; Sweden
- ⁹⁵ Centre de Calcul de l'Institut National de Physique Nucléaire et de Physique des Particules (IN2P3), Villeurbanne; France
- ⁹⁶ Departamento de Física Teórica C-15 and CIAFF, Universidad Autónoma de Madrid, Madrid; Spain
- ⁹⁷ Institut für Physik, Universität Mainz, Mainz; Germany
- ⁹⁸ School of Physics and Astronomy, University of Manchester, Manchester; United Kingdom
- ⁹⁹ CPPM, Aix-Marseille Université, CNRS/IN2P3, Marseille; France
- ¹⁰⁰ Department of Physics, University of Massachusetts, Amherst MA; United States of America
- ¹⁰¹ Department of Physics, McGill University, Montreal QC; Canada
- ¹⁰² School of Physics, University of Melbourne, Victoria; Australia
- ¹⁰³ Department of Physics, University of Michigan, Ann Arbor MI; United States of America
- ¹⁰⁴ Department of Physics and Astronomy, Michigan State University, East Lansing MI; United States of America
- ¹⁰⁵ B.I. Stepanov Institute of Physics, National Academy of Sciences of Belarus, Minsk; Belarus
- ¹⁰⁶ Research Institute for Nuclear Problems of Byelorussian State University, Minsk; Belarus
- ¹⁰⁷ Group of Particle Physics, University of Montreal, Montreal QC; Canada
- ¹⁰⁸ P.N. Lebedev Physical Institute of the Russian Academy of Sciences, Moscow; Russia
- ¹⁰⁹ National Research Nuclear University MEPhI, Moscow; Russia
- ¹¹⁰ D.V. Skobeltsyn Institute of Nuclear Physics, M.V. Lomonosov Moscow State University, Moscow; Russia
- ¹¹¹ Fakultät für Physik, Ludwig-Maximilians-Universität München, München; Germany
- ¹¹² Max-Planck-Institut für Physik (Werner-Heisenberg-Institut), München; Germany
- ¹¹³ Graduate School of Science and Kobayashi-Maskawa Institute, Nagoya University, Nagoya; Japan
- ¹¹⁴ Department of Physics and Astronomy, University of New Mexico, Albuquerque NM; United States of America
- ¹¹⁵ Institute for Mathematics, Astrophysics and Particle Physics, Radboud University/Nikhef, Nijmegen; Netherlands
- ¹¹⁶ Nikhef National Institute for Subatomic Physics and University of Amsterdam, Amsterdam; Netherlands
- ¹¹⁷ Department of Physics, Northern Illinois University, DeKalb IL; United States of America
- ¹¹⁸ ^(a) Budker Institute of Nuclear Physics and NSU, SB RAS, Novosibirsk; ^(b) Novosibirsk State University Novosibirsk; Russia
- ¹¹⁹ Institute for High Energy Physics of the National Research Centre Kurchatov Institute, Protvino; Russia
- ¹²⁰ Institute for Theoretical and Experimental Physics named by A.I. Alikhanov of National Research Centre "Kurchatov Institute", Moscow; Russia

- 121 Department of Physics, New York University, New York NY; United States of America
 122 Ochanomizu University, Otsuka, Bunkyo-ku, Tokyo; Japan
 123 Ohio State University, Columbus OH; United States of America
 124 Homer L. Dodge Department of Physics and Astronomy, University of Oklahoma, Norman OK; United States of America
 125 Department of Physics, Oklahoma State University, Stillwater OK; United States of America
 126 Palacký University, Joint Laboratory of Optics, Olomouc; Czech Republic
 127 Institute for Fundamental Science, University of Oregon, Eugene, OR; United States of America
 128 Graduate School of Science, Osaka University, Osaka; Japan
 129 Department of Physics, University of Oslo, Oslo; Norway
 130 Department of Physics, Oxford University, Oxford; United Kingdom
 131 LPNHE, Sorbonne Université, Université de Paris, CNRS/IN2P3, Paris; France
 132 Department of Physics, University of Pennsylvania, Philadelphia PA; United States of America
 133 Konstantinov Nuclear Physics Institute of National Research Centre “Kurchatov Institute”, PNPI, St. Petersburg; Russia
 134 Department of Physics and Astronomy, University of Pittsburgh, Pittsburgh PA; United States of America
 135 ^(a) Laboratório de Instrumentação e Física Experimental de Partículas – LIP, Lisboa; ^(b) Departamento de Física, Faculdade de Ciências, Universidade de Lisboa, Lisboa; ^(c) Departamento de Física, Universidade de Coimbra, Coimbra; ^(d) Centro de Física Nuclear da Universidade de Lisboa, Lisboa; ^(e) Departamento de Física, Universidade do Minho, Braga; ^(f) Departamento de Física Teórica y del Cosmos, Universidad de Granada, Granada (Spain); ^(g) Dep Física and CEFITEC of Faculdade de Ciências e Tecnologia, Universidade Nova de Lisboa, Caparica; ^(h) Instituto Superior Técnico, Universidade de Lisboa, Lisboa; Portugal
 136 Institute of Physics of the Czech Academy of Sciences, Prague; Czech Republic
 137 Czech Technical University in Prague, Prague; Czech Republic
 138 Charles University, Faculty of Mathematics and Physics, Prague; Czech Republic
 139 Particle Physics Department, Rutherford Appleton Laboratory, Didcot; United Kingdom
 140 IRFU, CEA, Université Paris-Saclay, Gif-sur-Yvette; France
 141 Santa Cruz Institute for Particle Physics, University of California Santa Cruz, Santa Cruz CA; United States of America
 142 ^(a) Departamento de Física, Pontificia Universidad Católica de Chile, Santiago; ^(b) Universidad Andres Bello, Department of Physics, Santiago; ^(c) Instituto de Alta Investigación, Universidad de Tarapacá, Arica; ^(d) Departamento de Física, Universidad Técnica Federico Santa María, Valparaíso; Chile
 143 Universidade Federal de São João del Rei (UFSJ), São João del Rei; Brazil
 144 Department of Physics, University of Washington, Seattle WA; United States of America
 145 Department of Physics and Astronomy, University of Sheffield, Sheffield; United Kingdom
 146 Department of Physics, Shinshu University, Nagano; Japan
 147 Department Physik, Universität Siegen, Siegen; Germany
 148 Department of Physics, Simon Fraser University, Burnaby BC; Canada
 149 SLAC National Accelerator Laboratory, Stanford CA; United States of America
 150 Department of Physics, Royal Institute of Technology, Stockholm; Sweden
 151 Departments of Physics and Astronomy, Stony Brook University, Stony Brook NY; United States of America
 152 Department of Physics and Astronomy, University of Sussex, Brighton; United Kingdom
 153 School of Physics, University of Sydney, Sydney; Australia
 154 Institute of Physics, Academia Sinica, Taipei; Taiwan
 155 ^(a) E. Andronikashvili Institute of Physics, Iv. Javakishvili Tbilisi State University, Tbilisi; ^(b) High Energy Physics Institute, Tbilisi State University, Tbilisi; Georgia
 156 Department of Physics, Technion, Israel Institute of Technology, Haifa; Israel
 157 Raymond and Beverly Sackler School of Physics and Astronomy, Tel Aviv University, Tel Aviv; Israel
 158 Department of Physics, Aristotle University of Thessaloniki, Thessaloniki; Greece
 159 International Center for Elementary Particle Physics and Department of Physics, University of Tokyo, Tokyo; Japan
 160 Department of Physics, Tokyo Institute of Technology, Tokyo; Japan
 161 Tomsk State University, Tomsk; Russia
 162 Department of Physics, University of Toronto, Toronto ON; Canada
 163 ^(a) TRIUMF, Vancouver BC; ^(b) Department of Physics and Astronomy, York University, Toronto ON; Canada
 164 Division of Physics and Tomonaga Center for the History of the Universe, Faculty of Pure and Applied Sciences, University of Tsukuba, Tsukuba; Japan
 165 Department of Physics and Astronomy, Tufts University, Medford MA; United States of America
 166 Department of Physics and Astronomy, University of California Irvine, Irvine CA; United States of America
 167 Department of Physics and Astronomy, University of Uppsala, Uppsala; Sweden
 168 Department of Physics, University of Illinois, Urbana IL; United States of America
 169 Instituto de Física Corpuscular (IFIC), Centro Mixto Universidad de Valencia – CSIC, Valencia; Spain
 170 Department of Physics, University of British Columbia, Vancouver BC; Canada
 171 Department of Physics and Astronomy, University of Victoria, Victoria BC; Canada
 172 Fakultät für Physik und Astronomie, Julius-Maximilians-Universität Würzburg, Würzburg; Germany
 173 Department of Physics, University of Warwick, Coventry; United Kingdom
 174 Waseda University, Tokyo; Japan
 175 Department of Particle Physics and Astrophysics, Weizmann Institute of Science, Rehovot; Israel
 176 Department of Physics, University of Wisconsin, Madison WI; United States of America
 177 Fakultät für Mathematik und Naturwissenschaften, Fachgruppe Physik, Bergische Universität Wuppertal, Wuppertal; Germany
 178 Department of Physics, Yale University, New Haven CT; United States of America

^a Also at Borough of Manhattan Community College, City University of New York, New York NY; United States of America.

^b Also at Bruno Kessler Foundation, Trento; Italy.

^c Also at Center for High Energy Physics, Peking University; China.

^d Also at Centro Studi e Ricerche Enrico Fermi; Italy.

^e Also at CERN, Geneva; Switzerland.

^f Also at CPPM, Aix-Marseille Université, CNRS/IN2P3, Marseille; France.

^g Also at Département de Physique Nucléaire et Corpusculaire, Université de Genève, Genève; Switzerland.

^h Also at Departament de Física de la Universitat Autònoma de Barcelona, Barcelona; Spain.

ⁱ Also at Department of Financial and Management Engineering, University of the Aegean, Chios; Greece.

^j Also at Department of Physics and Astronomy, Michigan State University, East Lansing MI; United States of America.

^k Also at Department of Physics and Astronomy, University of Louisville, Louisville, KY; United States of America.

^l Also at Department of Physics, Ben Gurion University of the Negev, Beer Sheva; Israel.

^m Also at Department of Physics, California State University, East Bay; United States of America.

ⁿ Also at Department of Physics, California State University, Fresno; United States of America.

^o Also at Department of Physics, California State University, Sacramento; United States of America.

- ^p Also at Department of Physics, King's College London, London; United Kingdom.
- ^q Also at Department of Physics, St. Petersburg State Polytechnical University, St. Petersburg; Russia.
- ^r Also at Department of Physics, University of Fribourg, Fribourg; Switzerland.
- ^s Also at Faculty of Physics, M.V. Lomonosov Moscow State University, Moscow; Russia.
- ^t Also at Faculty of Physics, Sofia University, 'St. Kliment Ohridski', Sofia; Bulgaria.
- ^u Also at Giresun University, Faculty of Engineering, Giresun; Turkey.
- ^v Also at Graduate School of Science, Osaka University, Osaka; Japan.
- ^w Also at Hellenic Open University, Patras; Greece.
- ^x Also at Institutio Catalana de Recerca i Estudis Avancats, ICREA, Barcelona; Spain.
- ^y Also at Institut für Experimentalphysik, Universität Hamburg, Hamburg; Germany.
- ^z Also at Institute for Particle and Nuclear Physics, Wigner Research Centre for Physics, Budapest; Hungary.
- ^{aa} Also at Institute of Particle Physics (IPP); Canada.
- ^{ab} Also at Institute of Physics, Azerbaijan Academy of Sciences, Baku; Azerbaijan.
- ^{ac} Also at Institute of Theoretical Physics, Iliia State University, Tbilisi; Georgia.
- ^{ad} Also at Instituto de Fisica Teorica, IFT-UAM/CSIC, Madrid; Spain.
- ^{ae} Also at Istanbul University, Dept. of Physics, Istanbul; Turkey.
- ^{af} Also at Joint Institute for Nuclear Research, Dubna; Russia.
- ^{ag} Also at Moscow Institute of Physics and Technology State University, Dolgoprudny; Russia.
- ^{ah} Also at National Research Nuclear University MEPhI, Moscow; Russia.
- ^{ai} Also at Physics Department, An-Najah National University, Nablus; Palestine.
- ^{aj} Also at Physikalisches Institut, Albert-Ludwigs-Universität Freiburg, Freiburg; Germany.
- ^{ak} Also at The City College of New York, New York NY; United States of America.
- ^{al} Also at TRIUMF, Vancouver BC; Canada.
- ^{am} Also at Università di Napoli Parthenope, Napoli; Italy.
- ^{an} Also at University of Chinese Academy of Sciences (UCAS), Beijing; China.
- ^{ao} Also at Yeditepe University, Physics Department, Istanbul; Turkey.
- * Deceased.